Courtship and Visual Defects of *cacophony* Mutants Reveal Functional Complexity of a Calcium-Channel α1 Subunit in Drosophila

Lee A. Smith,[1] Alexandre A. Peixoto,[2] Elena M. Kramer,[3] Adriana Villella and Jeffrey C. Hall

Department of Biology, Brandeis University, Waltham, Massachusetts 02254

Manuscript received January 24, 1998
Accepted for publication March 19, 1998

ABSTRACT

We show by molecular analysis of behavioral and physiological mutants that the Drosophila Dmca1A calcium-channel α1 subunit is encoded by the *cacophony* (*cac*) gene and that *nightblind-A* and *lethal(1)L13* mutations are allelic to *cac* with respect to an expanded array of behavioral and physiological phenotypes associated with this gene. The cac^{S} mutant, which exhibits defects in the patterning of courtship lovesong and a newly revealed but subtle abnormality in visual physiology, is mutated such that a highly conserved phenylalanine (in one of the quasi-homologous intrapolypeptide regions called IIIS6) is replaced by isoleucine. The cac^{H18} mutant exhibits defects in visual physiology (including complete unresponsiveness to light in certain genetic combinations) and visually mediated behaviors; this mutant (originally nbA^{H18}) has a stop codon in an alternative exon (within the *cac* ORF), which is differentially expressed in the eye. Analysis of the various courtship and visual phenotypes associated with this array of *cac* mutants demonstrates that Dmca1A calcium channels mediate multiple, separable biological functions; these correlate in part with transcript diversity generated via alternative splicing.

CALCIUM channels are involved in cellular functions such as regulation of membrane excitability, neurotransmission, and generation of rhythmic or bursting potentials (Hille 1992). Physiologically diverse channel subtypes are generated by multiple α1, α2δ, β and γ subunit genes, alternative splicing of transcripts from a given gene, and combinatorial assembly (reviewed by Hofmann *et al.* 1994; Stea *et al.* 1995). Six molecular classes of vertebrate α1 subunits have been cloned, and invertebrate α1 subunits have been cloned from Musca (Grabner *et al.* 1994), *Caenorhabditis elegans* (Schafer and Kenyon 1995; Lee *et al.* 1997), and Drosophila (Zheng *et al.* 1995; Smith *et al.* 1996). While much is known about molecular and physiological diversity of calcium channels, the biological role of calcium channel diversity is less well understood. Certain mammalian mutations (and an invertebrate one) offer hints at the biological functions of calcium channels (reviewed by Miller 1997). However, the defects associated with these calcium-channel variants are in the main neuropathologies, *e.g.*, migraines, ataxia, lethargy, and in one case muscular dysgenesis or myotonia; it is difficult to pit such mutant phenotypes against discrete, measurable behaviors exhibited by the wild-type humans, mice, or nematodes (*cf.* Schafer and Kenyon 1995; Lee *et al.* 1997; Miller 1997; and see the insightful discussion of this issue in Greenspan 1998).

We cloned the gene for the Drosophila Dmca1A calcium-channel α1 subunit and concluded from cDNA analysis that several variant isoforms were generated by alternative splicing (Smith *et al.* 1996; Peixoto *et al.* 1997). The Dmca1A-encoding gene spans several chromosomal breakpoints that fail to complement the courtship song defective *cacophony* (*cac*) mutation, the visually defective *nightblind-A* (*nbA*) mutations, and the *lethal(1)L13* mutations (Lindsley and Zimm 1992), suggesting that Dmca1A might be encoded by this gene or these genes.

Mutant alleles originally isolated as *nbA* strains lead to defects in visually mediated behaviors (Heisenberg and Götz 1975; Bülthoff 1982; Kulkarni and Hall 1987) and light-induced responses of the visual system (Heisenberg and Götz 1975; Coombe 1986; Coombe and Heisenberg 1986; Homyk and Pye 1989). These results stemmed from analyses of cac^{H18} (née nba^{H18}) and cac^{EE171} (née nba^{EE171}). An unpublished *nbA* mutant (now cac^{P73}, this article) was isolated in the lab of W. L. Pak (*cf.* Pak 1975) but was not extensively analyzed.

The courtship song of male *Drosophila melanogaster* is generated by wing vibration and has two components: sound "pulses" of 2–3 cycles each, repeated at approximately 35-msec intervals in trains of 2–30 pulses; and

Corresponding author: Jeffrey C. Hall, Department of Biology, MS-008, Brandeis University, 451 South Street, Waltham, MA 02254-9110. E-mail: hall@binah.cc.brandeis.edu

[1]*Present address:* Math and Science Division, College of San Mateo, 1700 West Hillsdale Boulevard, San Mateo, CA 94402.

[2]*Present address:* Fundação Oswaldo Cruz, Departamento de Bioquímica e Biologia Molecular, Rio de Janeiro 21045-900, Brazil.

[3]*Present address:* Department of Molecular, Cellular, and Developmental Biology, Yale University, P.O. Box 208104, New Haven, CT 06520-8103.

humming sounds (also called sine song, reviewed by Hall *et al.* 1980, 1990; Hall 1994). The cac^S mutation causes song pulses to be polycyclic and higher amplitude, with longer-than-normal intervals between pulses. This is exemplified in Figure 5 (within the discussion), mentioning of which also previews a connection we will make between changes in song patterns and more than one gene's worth of ion-channel variations. cac^S causes a depression of locomotor activity, but only at high temperatures, and does not affect sine song or the adult's ability to fly (Schilcher 1976, 1977; Kulkarni and Hall 1987; Wheeler *et al.* 1989; Peixoto and Hall 1998).

Mutations of *lethal(1)L13* (now $cac^{L\text{-}}$'s) cause late embryonic lethality in homozygotes (Perrimon *et al.* 1989) with no apparent anatomical defects (Perrimon *et al.* 1984). These lethal mutations fail to complement cac^S for song phenotypes; and most fail to complement cac^{EE171} for visual phenotypes (Kulkarni and Hall 1987; Homyk and Pye 1989), implying that the mutations are mutated at the same locus. However, one of these lethal mutations, $cac^{L\text{-}24}$, complements *nbA* mutations for all visual phenotypes but uncovers the song abnormalities associated with cac^S (this article). For its part, cac^S has not been demonstrably defective in visual functions; cac^{EE171} was found to be normal for courtship song; and cac^S and cac^{EE171} complemented each other for both song and visual phenotypes (Kulkarni and Hall 1987).

Nevertheless, the cytological localization, protein function, and transcript diversity of Dmca1A suggested that it might be the product of the *cac* gene. We have substantially extended and deepened the analysis of phenotypic interactions between *cac* alleles. Our results show that *cac* and *nbA* mutations are mutated with respect to the same function and indicate that the *cacophony* gene is involved in visual transduction as well as putative signal-transmission events that underlie the male's courtship song. In conjunction with these phenogenetic analyses, molecular characterization of mutations at this locus showed that cac^S carries a missense substitution at the site of a highly conserved phenylalanine residue; and cac^{H18} (which affects visual but not song phenotypes) is a nonsense mutant, predicted to eliminate expression of an alternative exon that is differentially expressed in the eye.

MATERIALS AND METHODS

Reverse transcription (RT)-PCR: Total RNA for each genotype was isolated with TRIzol reagent (GIBCO BRL, Gaithersburg, MD) from intact adult flies. Total RNA (1.5 μg) was reverse-transcribed with random hexamer primers and AMV Reverse Transcriptase (Promega, Madison, WI) and then amplified for sequence analysis by nested PCR. All PCRs were in 100-μl volumes and included the following: 0.2 μm each primer; 0.2 mm each dNTP; 1.75 mm $MgCL_2$; 50 mm KCl; 10 mm Tris-HCl, pH 9.0; 0.1% Triton X-100; and 5 units Taq polymerase. Primary PCRs—designed to amplify 1.5–2-kb products, containing 2 μl of cDNA template (from a 1:100 dilution of the first-strand cDNA)—were denatured at 94° for 2 min and subjected to 20 amplification cycles (94°, 1 min; 59°, 1 min; 72°, 2 min), followed by 5 min at 72°. Secondary nested PCRs were prepared as above (except that they were designed to amplify 380–1250-bp products), contained 5 μl of the first-round PCR product as template, and were given 40 cycles (94°, 1 min; 59° 1 min; 72°, 1 min).

PCR from genomic DNA: To extract genomic DNA for PCR, single flies were homogenized in 50 μl of "squishing buffer" (10 mm Tris/HCl, pH 8.2, 1 mm EDTA, 25 mm NaCl, 200 μg/ml Proteinase K), incubated 30 min at room temperature, and heated to 95° for 2 min. PCRs contained 2–4 μl of fresh extracted DNA, amplified 40 cycles (94°, 1 min; 59°, 1 min; 72°, 1 min), and were otherwise identical to those above. PCR primers were designed to genomic DNA flanking exon I/IIa, and had the sequences: (B5′-2) 5′-CCC AAA TTT TCG CCT GTT GC-3′; (B3′-2) 5′-GGT TGT GTT GTA TGA CGT TCG-3′. Control PCRs contained no template DNA.

Sequencing and analysis of resulting data: PCR products were purified with the QIAquick PCR Purification Kit (Qiagen, Santa Clarita, CA) and eluted in 25 μl H_2O. Typically, 9.5 μl of eluant was sequenced using the ABI PRISM Dye-Deoxy Terminator Cycle Sequencing Kit (Perkin Elmer, Foster City, CA) and electrophoresed on an ABI 373A automated sequencer. Sequence analysis was done with GCG sequence analysis software (Genetics Computer Group 1991). Ambiguities were resolved by direct reference to the sequence chromatograph. At several sites, RT-PCR derived sequence did not allow unambiguous identification of nucleotide identity; nucleotides at these sites were considered not to be polymorphic if the chromatographic pattern from each of the different strains was similar and consistent with the published Dmca1A sequence. Silent third-base polymorphisms were detected at seven sites in the Dmca1A transcript; we interpret these as strain differences. All polymorphisms were confirmed by subsequent RT-PCR-sequencing analyses ($n \geq 3$) from RNA independently purified from the relevant fly strain.

Mutants and other genetic variants: All abnormal genotypes are listed in Lindsley and Zimm (1992). Most of these variants involve the *X*-chromosomal *cacophony* locus (see below). Others included the sightless *no-receptor-potenital-A* ($norpA^{P24}$) and *eyes-absent* (eya^1) mutants. cac^{P73} (née nbA^{P73}) was obtained from W. L. Pak. Flies were maintained at 25°, 70% relative humidity, and those to be tested in behavioral or physiological experiments were collected under CO_2 anesthesia within 24 hr of eclosion and aged for 3–7 days before testing. All viable *cac* mutant and wild-type strains used for analysis were subjected to a five-generation outcross to a common stock marked with $vermilion^2$, $garnet^2$, and *forked* ($v^2\ g^2\ f$). Several separately-maintained cac^S lines, initially expressing significantly different numbers of cycles per pulse (CPP) and interpulse internal (IPI) scores (see below), converged to common, mutant values during the outcrossing, indicating that genetic variability affecting these parameters had been removed. To guard against subsequent selection for genetic modifiers that might again cause phenotypic drift, the outcrossed viable mutants were crossed into and maintained in stocks with an attached-*XY* chromosome (*FM7-Y*; also known as $Y^SX\text{-}Y^L$, *In(1)FM7*: Lindsley and Zimm 1992). The only fertile flies in these stocks are *FM7-Y* males and heterozygous females, which do not express recessive phenotypes, minimizing the accumulation of modifying factors that can degrade the severity of the behavioral phenotypes (*cf.* de Belle and Heisenberg 1996). Lethal *cac* alleles were crossed to the $v^2\ g^2\ f$ stock, then reisolated by crossing to a balancer stock [*In(1)FM7*] that had been outcrossed to the strain indicated above. Flies for visual-behavior or ERG tests (see below) were obtained by crosses from

these stocks. Flies for courtship-song analysis were obtained by first crossing the relevant *cac*-mutant or cac^+-containing stocks to flies from a single stock containing *transformer* (*tra*) mutation—which when homozygous transforms diplo-*X*, chromosomally female flies into phenotypic pseudomales that robustly perform male-specific behaviors (*e.g.*, Bernstein *et al.* 1992) and subsequently crossing the resulting progeny together to produce *cac*-heteroallelic diplo-*X*, homozygous *tra* pseudomales.

Courtship-song analysis: The recording and analytical procedures were essentially as described by Rendahl *et al.* (1992). Males or pseudomales were stored individually for 3–7 days after eclosion. Each fly was then placed with one or two attached-*X* [*C(1)DX, y f*] females in the recording chamber of an Insectavox (Gorczyca and Hall 1987). Five minutes of courtship were recorded on a Sony (Parkridge, NJ) Hi-8 audio-video recorder. The analog sound record was transferred at 2000 Hz via MacAdios II analog-digital converter to a Macintosh II or Quadra computer. Song-pulse locations were marked using LifeSong software (Bernstein *et al.* 1992) and subsequently analyzed on a VAX 8650. The values associated with pulse-song parameters for a given genotype are the means among individuals, computed from the means determined for each individual's 5 min of recorded courtship. The parameters extracted from the analyses were IPIs (*e.g.*, Schilcher 1976, 1977; Rendahl *et al.* 1992; Peixoto and Hall 1998), CPPs (*e.g.*, Kulkarni and Hall 1987; Bernstein *et al.* 1992; Rendahl *et al.* 1992), intrapulse (or carrier) frequencies (*e.g.*, Wheeler *et al.* 1989; Bernstein *et al.* 1992; Rendahl *et al.* 1992), and amplitude of pulses (in arbitrary units; *cf.* Peixoto and Hall 1998). Recordings were obtained at temperatures between 20–25°; the IPI varies with temperature, with a slope of 1.74 msec/° (Ritchie and Kyriacou 1994); thus IPI values were corrected using this relationship to a standard temperature of 22°.

Visually mediated behaviors: The walking optomotor assay was performed in a rotating arena essentially as described by Rendahl *et al.* (1992) and references therein. Each fly was given six consecutive 1-min trials with alternating clockwise and counterclockwise rotation of the arena. The number of times a given fly crossed a quadrant line in the same direction as a rotating background (F), or in the opposite direction (B), were totaled. An "optomotor index" was calculated with the formula $(F - B)/(F + B)$, yielding a score of one if the fly always followed the rotating background, and a score of zero if the fly was equally likely to move either direction.

A "countercurrent-regression" assay was devised to test the ability of flies to phototax under varying light intensities. A five-tube countercurrent phototaxis apparatus (Benzer 1967) was placed 10 cm from a light source (General Electric 18-W fluorescent bulb) equipped with light filters (Rosco N.6 2-stop neutral density). Approximately 35–50 flies were introduced into the proximal tube of the apparatus, tapped to the bottom, and allowed to distribute themselves between the proximal and distal tubes for 30 sec. The apparatus was then shifted and tapped to return the flies to the proximal tube. This was repeated five times, fractionating the flies into six groups based on the number of transitions toward light (0–5) by each. A "transition score" was calculated, representing for each group the number of actual transitions toward light as a fraction of the total possible. The procedure was repeated in the dark and with filtered light intensities of 0.1 f.c., 1.4 f.c., and 340 f.c. Parallel tests of wild-type and several mutant lines in constant darkness or constant 340-f.c. light detected no fatigue effects from the multiple trials. Transition scores were regressed against light intensity. Positive regression slopes indicate increased phototaxis in increasing light intensities, and negative slopes indicate decreased phototaxis.

Y-tube phototaxis was performed as described by Kulkarni and Hall (1987). Flies were placed in a darkened start tube and then exposed for 120 sec to a choice point allowing access to either a dark tube or a tube with a light source at the distal end. The number of flies choosing the lighted (L) or darkened (D) tubes was counted, and a phototaxis index with values between minus one and one was calculated using the formula $(L - D)/(\text{total flies})$; positive scores indicate a preference for the lighted tube, and negative scores for the dark tube.

Electroretinograms (ERGs): ERGs were recorded as described by Rendahl *et al.* (1992). All test recordings were preceded and followed by recordings of wild-type flies; only if both control recordings were normal was the test ERG accepted for analysis. The absolute amplitude in mV of the light-on and light-off transient spikes [from baseline and from the end of the light coincident receptor potential (LCRP), respectively] and the maximum amplitude of the LCRP were measured, as well as the time between light-on and the maximal absolute LCRP amplitude.

Statistics: These analyses were performed by application of JMP software (SAS Institute 1994). Optomotor and Y-tube scores were transformed to arcsin[score], countercurrent-regression, ERG and song scores except CPP were transformed with 1/[score], and CPP scores with 1/sqrt[score], yielding homogeneity of variances (Sokal and Rohlf 1995). ANOVA for each assay gave a P[equivalent means] of $<<0.001$. Genotypes were subsequently tested for equivalence to wild type (Dunnett 1955), and also for equivalence to sightless $norpA^{P24}$ and eya^1 control flies (visual behavior) or to cac^S hemizygous mutant males (song). These parametric methods were supplemented with Wilcoxon/Kruskal-Wallis nonparametric pairwise comparison tests (see legends to Tables 1 and 2).

Northern blotting: Drosophila heads and bodies were separated by sieving in liquid nitrogen (Levy and Manning 1981). Total RNA was isolated using TRIzol reagent (GIBCO BRL). Poly(A)$^+$ RNA was purified with the PolyATtract mRNA Isolation System (Promega). PolyA$^+$ RNA (3.5 μg) was loaded in each lane, electrophoresed through a 1% agarose/formaldehyde gel, and transferred onto a Hybond-N$^+$ membrane as described by the manufacturer (Amersham, Arlington Heights, IL). Probe (2×10^6 cpm/ml) was generated by random-primed ^{32}P-labeling of a 682-bp PCR fragment generated from cDNA clone cSK53 (Smith *et al.* 1996) with primers U857 (5′-CCG AAA TTG AAA GCC GTG TT-3′) and L1522 (5′-ACT TCA TCA TCA GCA ATA GG-3′), corresponding to amino acids 889 (C-terminal end of IIIS4) through 1116 (C-terminal end of IVS1). The lower portion of each blot was removed and probed with 2×10^6 cpm/ml of an *rp49* probe (O'Connell and Rosbash 1984) as a control for equal loading. The Dmca1A portion was exposed to film for 9 days and the *rp49* portion, for 5 hr.

Tissue-specific RT-PCR: Isolation of RNA and reverse transcription was performed as above, except that 0.25 μg of total RNA from eyes was reverse-transcribed, with reagents scaled proportionally. Eyes were isolated by freezing flies in liquid nitrogen, transferring to ethanol on dry ice, and "popping" the eyes off with a fine tungsten needle. A single-step PCR in 100 μl total volume was performed as above, with 2 μl of template cDNA, an annealing temperature of 61°, and amplification for 30 cycles. Primer sequences (applied in the experiments depicted in Figure 4) were designed to give products between 188 and 250 bp in length: (A) 5′-CCA TGT TTC AGA CAG CAA TGG-3′; (B) 5′-GTA CGA GAC CAT TGC TGT CTG-3′; (C) 5′-CCT AAA CTT AGA AGG CAG CAG C-3′; (D) 5′-CGA ATT CAC CAC TAA GGA CAC C-3′, (5′) 5′-TGA CCG TAT TCC AAT GTA TC-3′, (3′) 5′-CTT CCT CTT CCT CTG TAT-3′.

Preliminary titrations using cDNA dilutions of 1:1, 1:10,

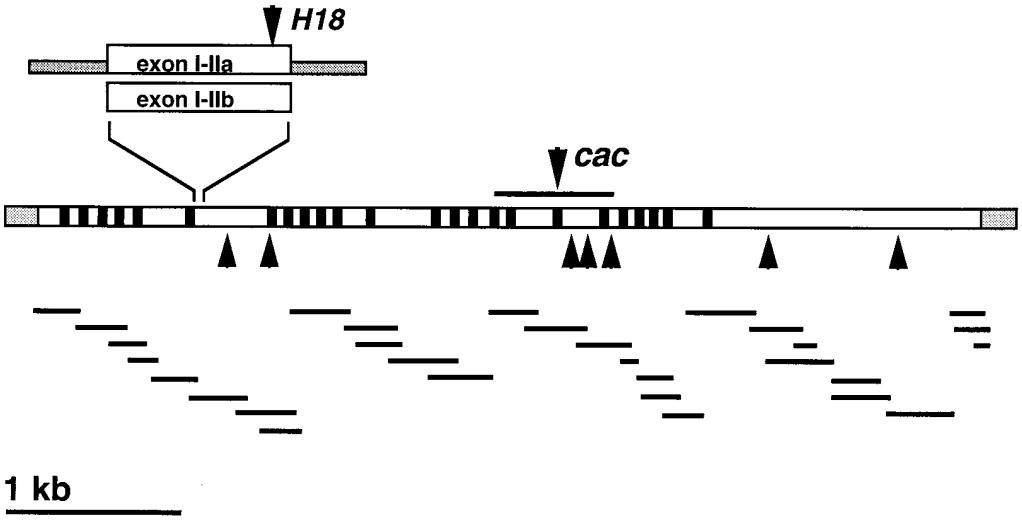

Figure 1.—Sequence analysis of Dmca1A transcripts. The products of the *cac* gene are diagrammed, with locations of transmembrane domains of the Dmca1A polypeptide indicated by vertical black bars; untranslated regions (UTR) of the transcript are in gray. Mutually exclusive 118-bp alternative exons in the domain I-II loop (exons I-IIa and I-IIb) are expanded 10×; sequences from introns flanking exon I-IIa are indicated in gray. The horizontal line above the diagram indicates the probe used on Northern blots (Figure 4). Sequence fragments obtained from *cac* mutants by RT-PCR are indicated by horizontal lines underneath the diagram; diagonally descending sets derive from the same primary PCR. Unlabeled arrows indicate the positions of silent polymorphisms. Labeled arrows indicate nonsilent polymorphisms in the indicated mutant flies (*H18*, cac^{H18}).

1:100, and 1:1000 showed that dilutions of <1:10 were subsaturating for PCR amplification of each product (Huet *et al.* 1993); subsequent experiments were done with 1:100 dilutions for primer pairs A and B and 1:250 dilutions for primer pairs C and D. Each PCR (10 μl) was electrophoresed on 2% agarose gels, stained with Ethidium Bromide, and photographed under UV illumination. Representative examples of each size class were purified and sequenced as described in results.

RESULTS

Nucleotide substitutions in *cac* mutants: The Dmca1A open reading frame (ORF) is diagrammed in Figure 1; it also depicts the basic structure of this calcium-channel subunit and its four quasi-repeated domains, each containing six transmembrane regions. We sequenced the Dmca1A ORF (by RT-PCR, as outlined in Figure 1) from four viable mutants: cac^{S}, cac^{H18}, cac^{EE171}, and cac^{P73}. Except as noted with respect to sites associated with certain *cac* mutations (Figure 1), the sequences obtained from these four previously unanalyzed strains were identical to the known informational content of Dmca1A (*cf.* Smith *et al.* 1996; Peixoto *et al.* 1997).

One proviso that must accompany the statement just made involves post-transcriptional modification of certain adenosine residues within the Dmca1A ORF. We had found that certain sites exhibit heterogeneity (among cDNAs) in terms of the nucleotides present at these sites (Smith *et al.* 1996; Peixoto *et al.* 1997). That the nucleotides were either adenosine or guanosine (and other arguments) suggested strongly that these sites are subjected to "A-to-G" RNA editing (see Smith *et al.* 1996, 1998, for evidence and discussion; as well as Simpson and Emeson 1996, for background information). The current point is that the same kind of A/G heterogeneity was detected at the relevant sites in cDNAs derived from all four mutants (data not shown), as found in the pattern previously established for wild type.

The molecular etiology of two *cac* mutants seems to involve a straightforward missense and an intriguing nonsense mutation, respectively: A single transversion in sequence encoding transmembrane domain IIIS6 was the only nonsilent polymorphism detected in cac^{S} mutant flies (Figure 2A). This nucleotide substitution changes a phenylalanine codon (TTC) to an isoleucine one (ATC). Given the current knowledge of alternative splicing of Dmca1A's primary transcript (Smith *et al.* 1996), the amino-acid substitution in cac^{S} would be expected to affect all of the mature transcript types. The affected phenylalanine is perfectly conserved among calcium channel α1 and sodium channel α subunits (Figure 2C), and in the transmembrane domain region of the MinK subunit of I_{kS} potassium channels (Wang *et al.* 1996); this I_{kS} transmembrane region can be aligned with transmembrane domain IIIS6 of Na^{+} α and Ca^{2+} α1 channel subunits but is otherwise quite diverged (Takumi *et al.* 1988; Barhanin *et al.* 1996; Sanguinetti *et al.* 1996). The cac^{S}-defined phenylalanine is not conserved in S6 transmembrane domains of six-transmembrane-domain potassium channels (see discussion).

Dmca1A has mutually exclusive alternative exons (I/IIa and I/IIb) that encode a portion of the intracellular

loop between homologous repeats I and II (Smith *et al.* 1996) (Figure 2D). Exon I/IIb of Dmca1A encodes a sequence motif that mediates interaction with calcium channel β-subunits and is conserved in all α1 subunits (Pragnell *et al.* 1994). Exon I/IIb also encodes an overlapping sequence, present in a subset of α1 subunits, which mediates modulation by G-protein $G_{\beta g}$ subunits (Zhang *et al.* 1996; De Waard *et al.* 1997; Herlitze *et al.* 1997a,b; Zamponi *et al.* 1997). The alternative Dmca1A exon I/IIa encodes a sequence that has poor conservation of the β-subunit-interaction motif and does not have the $G_{\beta\gamma}$ interaction motif.

Exon I/IIb was readily amplified and sequenced from RT-PCR templates, but exon I/IIa was amplified at a reduced level. Exon I/IIa, along with 64 flanking 5′ nucleotides and 56 flanking 3′ nucleotides, was amplified and sequenced from genomic DNA. A single transition was found near the 3′ end of exon I/IIa in cac^{H18} (Figure 2B), altering a tryptophan codon to a TAG amber stop codon (Figure 2D). This nonsense substitution was the only nonsilent sequence polymorphism detected in the cac^{H18} ORF. The nucleotide substitution would cause premature termination and eliminate expression of Dmca1A isoforms containing the relatively unconserved amino-acid sequence encoded by exon I/IIa.

We did not find molecular lesions in the ORFs of cac^{EE171} or cac^{P73} mutants. Possible explanations for this could be that these are mutations outside the ORF and might affect spatial or temporal regulation or alternative splicing of Dmca1A isoforms necessary for visual function. While we have no evidence for additional Dmca1A alternative exons or for alternative translation initiation sites (see Smith *et al.* 1996; Peixoto *et al.* 1997), we cannot discount the existence of such molecular entities as being involved in visual system function. Given that cac^{H18} is mutated in alternative exon I/IIa, that cac^{H18} mutants are defective only in vision, and that $cac^{L\text{-}24}$ has no vision defects, we predicted that the $cac^{L\text{-}24}$ mutation

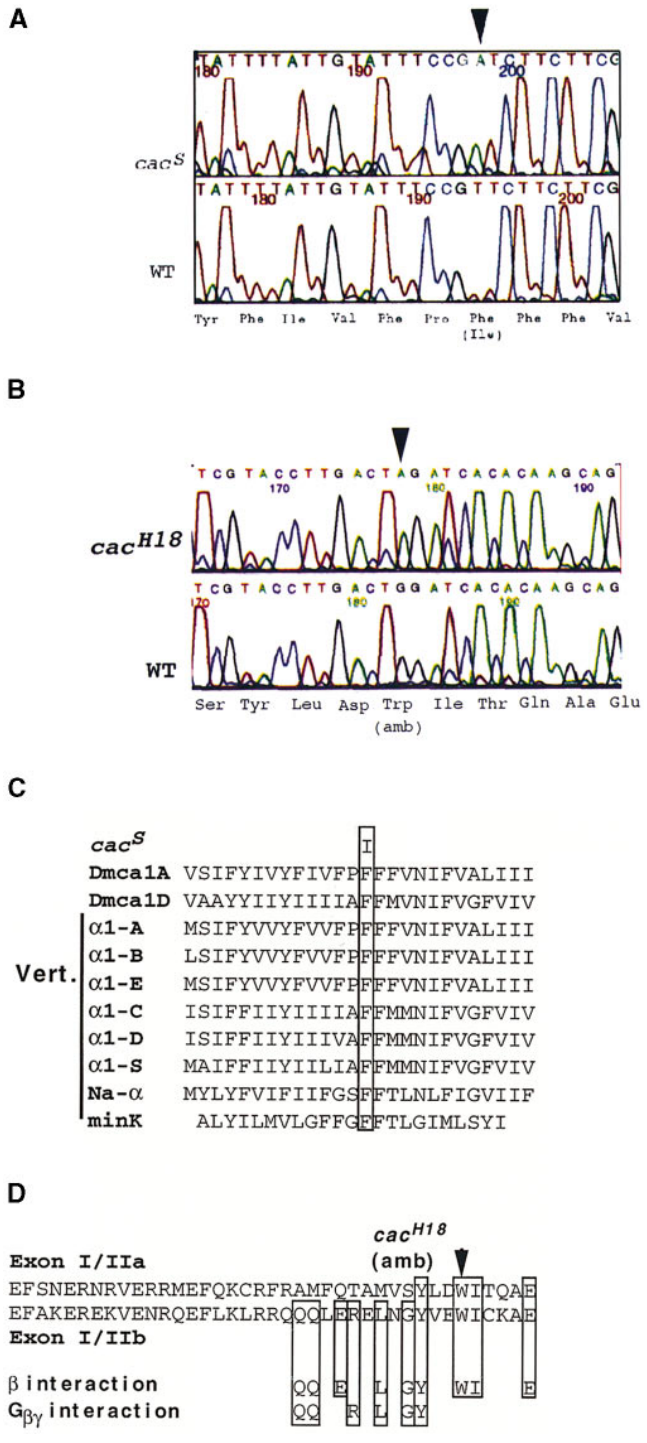

Figure 2.—Mutations affecting the Dmca1A calcium-channel α1 subunit. (A) cac^{S} mutant flies have a TTC-Phe to ATC-Ile change; the arrow indicates the variant nucleotide in cac^{S}; the protein sequence is aligned below the chromatographs, with the cac^{S} variant in parentheses. (B) cac^{H18} mutant flies have a TGG-Trp to TAG-stop change in exon I/IIa; the arrow indicates the variant nucleotide in cac^{H18} mutant flies; the protein sequence is shown aligned below the chromatographs, with the cac^{H18}-variant stop codon in parentheses. (C) The cac^{S} mutation affects a conserved phenylalanine in transmembrane domain IIIS6; the Dmca1A calcium-channel sequence is aligned with representative calcium-channel, sodium-channel, and minK potassium-channel sequences; the phenylalanine affected by this Drosophila mutation is boxed; the channels in other species are as follows: α1A, rat brain class A (GenBank accession no. M64373; Starr *et al.* 1991); α1B, rat brain class B (GenBank accession no. M92905; Dubel *et al.* 1992); α1E, rat brain class E (GenBank accession no. M94172; Soong *et al.* 1993); α1C, rat brain class C (GenBank accession no. M67516; Snutch *et al.* 1991); α1D, human class D (GenBank accession no. M76558; Williams *et al.* 1992); α1S, rat skeletal muscle (GenBank accession no. X05921; Tanabe *et al.* 1987). (D) The cac^{H18} mutation creates a stop codon in exon I/IIa; the location of the stop codon is indicated with an arrowhead; sequences known to be important in β-subunit interaction (Pragnell *et al.* 1994) and in Gβγ-mediated channel modulation of vertebrate α1 subunits (Zhang *et al.* 1996; De Waard *et al.* 1997; Herlitze *et al.* 1997a,b; Zamponi *et al.* 1997) are aligned below the exon sequences, with conserved amino acids boxed.

TABLE 1

Courtship-song components

Genotype	*n*	IPI (sec)	CPP (No.)	Amplitude (arbitrary units)
1/1	6	0.042 ± 0.001	2.79 ± 0.12	13.1 ± 0.6
	4	0.046 ± 0.001	3.23 ± 0.11	60.8 ± 11.2
1/3	6	0.044 ± 0.001	2.83 ± 0.11	11.3 ± 0.5
	3	0.044 ± 0.001	3.27 ± 0.18	103.1 ± 17.7
1/4	7	0.043 ± 0.001	2.94 ± 0.11	12.7 ± 0.6
	3	0.043 ± 0.002	2.49 ± 0.09	51.8 ± 8.9
3/3	6	0.042 ± 0.001	2.79 ± 0.14	11.4 ± 0.6
	4	0.044 ± 0.001	3.30 ± 0.15*	88.3 ± 22.4
3/4	6	0.043 ± 0.000	2.74 ± 0.13	11.4 ± 0.5
	3	0.043 ± 0.001	3.11 ± 0.48	119.7 ± 17.7
4/4	6	0.042 ± 0.000	3.05 ± 0.09	12.9 ± 0.3
1/*Df*	6	0.041 ± 0.000	3.09 ± 0.19	11.6 ± 0.2
1/*L-6*	6	0.044 ± 0.001	3.17 ± 0.07	14.0 ± 0.4
	2	0.045 ± 0.001	3.83 ± 0.05*	128.7 ± 4.3
1/*L-10*	7	0.041 ± 0.000	3.06 ± 0.08	13.8 ± 0.2
	3	0.046 ± 0.002	3.49 ± 0.12*	104.9 ± 15.1
1/*L-13*	8	0.047 ± 0.001	3.42 ± 0.13	13.7 ± 0.6
	4	0.048 ± 0.007*	3.18 ± 0.16	94.6 ± 18.2
1/*L-20*	7	0.045 ± 0.001	3.00 ± 0.07	12.2 ± 0.6
	3	0.045 ± 0.002	3.88 ± 0.05*	131.8 ± 18.2
1/*L-24*	6	0.043 ± 0.001	3.21 ± 0.13	13.6 ± 0.4
	4	0.045 ± 0.002	2.92 ± 0.27	102.2 ± 21.6
3/*Df*	6	0.041 ± 0.000	2.95 ± 0.06	12.1 ± 0.4
3/*L-6*	6	0.045 ± 0.001	3.21 ± 0.15	12.6 ± 0.5
	3	0.044 ± 0.001	3.39 ± 0.03*	79.1 ± 3.5
3/*L-10*	6	0.045 ± 0.000	3.08 ± 0.07	13.0 ± 0.4
	2	0.052 ± 0.000*	3.76 ± 0.24*	102.1 ± 12.0
3/*L-13*	6	0.045 ± 0.001	3.06 ± 0.13	12.3 ± 0.8
	2	0.050 ± 0.004*	3.44 ± 0.05*	102.3 ± 8.1
3/*L-20*	7	0.046 ± 0.001	3.03 ± 0.10	12.2 ± 0.4
	2	0.047 ± 0.002	3.39 ± 0.17	87.9 ± 21.1
3/*L-24*	6	0.048 ± 0.001	3.11 ± 0.18	11.5 ± 0.5
	2	0.048 ± 0.001*	2.91 ± 0.17	86.1 ± 4.0
4/*Df*	6	0.042 ± 0.001	3.38 ± 0.15	15.4 ± 1.0*
4/*L-6*	9	0.044 ± 0.001	3.48 ± 0.26	14.5 ± 1.5*
	3	0.045 ± 0.001	3.96 ± 0.05*	53.2 ± 3.1
4/*L-10*	7	0.045 ± 0.001	2.99 ± 0.07	13.9 ± 0.6
	3	0.044 ± 0.001	2.65 ± 0.10	59.9 ± 4.7
4/*L-13*	7	0.046 ± 0.001	3.38 ± 0.14	14.8 ± 1.2*
	3	0.051 ± 0.004*	3.42 ± 0.27*	96.5 ± 11.7
4/*L-20*	6	0.043 ± 0.001	2.78 ± 0.15	14.9 ± 0.8*
	3	0.044 ± 0.000	3.66 ± 0.09*	88.5 ± 4.2
4/*L-24*	8	0.044 ± 0.001	3.44 ± 0.15	13.6 ± 0.6
	3	0.047 ± 0.001*	2.99 ± 0.31	107.7 ± 31.1
cac/1	7	0.045 ± 0.001	3.21 ± 0.15	13.5 ± 0.3
	3	0.045 ± 0.001	2.32 ± 0.10	44.4 ± 6.1
cac/3	6	0.042 ± 0.001	3.13 ± 0.14	13.9 ± 0.5
	3	0.042 ± 0.002	2.54 ± 0.28	52.0 ± 15.4
cac/4	7	0.042 ± 0.001	3.47 ± 0.10	16.3 ± 0.6**
	2	0.043 ± 0.001	2.63 ± 0.28	72.5 ± 5.1
cac/*cac*	7	0.057 ± 0.001**	4.76 ± 0.20**	17.0 ± 0.6**
	4	0.057 ± 0.000**	5.13 ± 0.04**	151.8 ± 11.4
cac/*Df*	9	0.056 ± 0.001**	4.84 ± 0.17**	17.2 ± 0.9**
cac/*L-6*	6	0.057 ± 0.002**	4.80 ± 0.18**	16.7 ± 0.7**
	3	0.064 ± 0.001**	4.52 ± 0.14**	204.4 ± 33.7

(*continued*)

TABLE 1

Continued.

Genotype	*n*	IPI (sec)	CPP (No.)	Amplitude (arbitrary units)
cac/*L-10*	6	0.056 ± 0.002**	4.73 ± 0.30**	15.9 ± 0.9**
	5	0.056 ± 0.001**	5.20 ± 0.38**	161.9 ± 13.3
cac/*L-13*	6	0.053 ± 0.001**	4.57 ± 0.32**	15.5 ± 1.3**
	3	0.055 ± 0.002**	4.88 ± 0.43**	171.3 ± 22.5
cac/*L-20*	6	0.051 ± 0.002**	4.56 ± 0.62**	18.0 ± 1.2**
	3	0.061 ± 0.001**	5.23 ± 0.34**	207.4 ± 17.6
cac/*L-24*	7	0.051 ± 0.002**	4.09 ± 0.34**	5.4 ± 1.1**
	4	0.059 ± 0.002**	5.97 ± 0.31**	177.2 ± 33.0
WT/1	6	0.042 ± 0.001	3.12 ± 0.07	12.7 ± 0.5
	3	0.045 ± 0.000	2.62 ± 0.26	88.4 ± 23.0
WT/3	6	0.044 ± 0.001	2.98 ± 0.12	12.8 ± 0.3
	3	0.045 ± 0.001	3.51 ± 0.47*	127.0 ± 25.4
WT/4	6	0.043 ± 0.001	3.16 ± 0.12	14.1 ± 0.9
	4	0.044 ± 0.000	2.86 ± 0.11	67.1 ± 4.9
WT/*cac*	6	0.050 ± 0.003*	3.78 ± 0.43*	14.4 ± 1.2*
	4	0.048 ± 0.001*	3.72 ± 0.16*	103.5 ± 12.5
WT/*Df*	8	0.042 ± 0.001	3.10 ± 0.12	14.5 ± 1.5*
WT/*L-6*	7	0.043 ± 0.001	3.07 ± 0.09	12.2 ± 0.9
	3	0.046 ± 0.000	3.25 ± 0.03	90.2 ± 4.5
WT/*I-10*	6	0.044 ± 0.001	3.35 ± 0.11	14.2 ± 0.5
	2	0.040 ± 0.001	3.23 ± 0.16	83.4 ± 13.0
WT/*L-13*	6	0.048 ± 0.002	3.44 ± 0.15	11.8 ± 0.7
CS/*L-13*	6	0.044 ± 0.001	2.99 ± 0.09	12.2 ± 0.8
	3	0.049 ± 0.001*	3.21 ± 0.25	79.6 ± 7.5
WT/*L-20*	7	0.044 ± 0.001	2.98 ± 0.06	10.6 ± 0.6
	4	0.042 ± 0.000	2.98 ± 0.14	100.7 ± 8.8
WT/*L-24*	5	0.042 ± 0.001	3.51 ± 0.02	14.3 ± 0.3
CS/*L-24*	6	0.044 ± 0.001	2.91 ± 0.11	12.4 ± 0.7
	3	0.042 ± 0.000	2.99 ± 0.11	119.8 ± 9.3
WT/CS	7	0.046 ± 0.001	2.99 ± 0.14	12.3 ± 0.7
WT/WT	4	0.045 ± 0.001	2.88 ± 0.16	13.4 ± 1.9
	4	0.041 ± 0.001	2.43 ± 0.12	80.4 ± 6.0

The acoustic parameters measured are as follows: Interpulse interval (IPI), cycles per pulse (CPP), and pulse amplitude. The *cac* genotype designations follow Lindsley and Zimm (1992): "*cac*", cac^{S}; "1", cac^{H18}; "3", cac^{EE171}; "4", cac^{P73}. For genotypes with two values, the lower entry is from a pilot experiment, and the upper is from a larger partially independent experiment. The two experiments were found by ANOVA to have a significant interaction component for all parameters ($P < 0.01$ in all cases), so the results are reported separately. The two experiments yield results largely consistent with each other, although several genotypes indicated as intermediate in the pilot experiment were not confirmed as such in the subsequent larger experiment. Default recording gain levels varied within the first experiment; this caused the pulse amplitude (calculated relative to an arbitrary standard during the computerized analysis) to vary within the first experiment, and these values are therefore not tabulated. WT designates an *X* chromosome derived from a wild-type stock that was rendered essentially isogenic with the mutant strains, except at the *cac* locus. Some *cac* genotypes were tested with an additional cac^{+} chromosome, CS, derived from a Canton-S wild-type strain in our laboratory; this was not isogenic with the other variants but was simply crossed to the *cac*-variant or WT flies to generate the genotypes indicated. *n*, number of flies recorded; **, statistically indistinguishable from cac^{S} mutant; *, "intermediate" values distinct from both ($\alpha = 0.01$); unmarked entries indicate values that are indistinguishable from wild type. The IPI results were confirmed by the nonparametric statistical tests (see materials and methods), except that there was a cleaner distinction between *cac*-like and normal values (no intermediate cases). Nonparametric and parametric tests of the CPP values led to essentially the same conclusions, except that 1/*L-13*, 4/*L-24*, and *cac*/4 were also different from wild type. Nonparametric tests involving amplitude again came out nearly the same as the other statistical tests, except that WT/1 was *cac*-like, and 1/*L-10* was different from wild type.

might be in exon I/IIb. However, sequence analysis of this alternative exon from cac^{L-24} mutants did not reveal any sequence polymorphisms (not shown). This could imply the existence of additional alternative Dmca1A transcripts that are not involved in visual processes.

To delve into those processes, and the courtship-song

ones as well, we now turn to the phenogenetics of *cacophony*. The results that follow are sometimes less accessible than the molecular findings. Nevertheless, we believe that the behavioral and physiological defects exhibited by the several *cac*-mutant combinations—involving discrete as well as graded phenotypic impairments—are crucial for revealing both that *cac* mutations define an allelic series and how the channel subunit encoded by this gene participates in distinct features of CNS and PNS function.

Courtship-song defects are associated with a subset of *cac* mutants: The original *cacophony* song mutant was found to generate anomalously polycyclic "tone pulses" (for example, Figure 5). To determine better whether further mutations at this locus cause these kinds of pulse abnormalities—or additional or other ones—we analyzed several song parameters beyond that involving number of cycles per pulse. The flies whose courtship wing vibrations were recorded represented all viable genotypic combinations of *cac* alleles, as well as those that are lethally mutated at or deleted of the *cac* locus (see materials and methods). These diplo-*X* (chromosomally female) flies were rendered phenotypically male by use of the *transformer* mutation (*cf.* Kulkarni and Hall 1987; Bernstein *et al.* 1992). The behavioral results were compared to those from wild-type flies and cac^S homozygotes (Table 1; summarized in Table 4). Elements of these phenogenetic results (here, and in the next three sections) are complex, but we hope the reader will bear with us.

The cac^S mutant types—carrying that allele as their only *cac* one, or cac^S heterozygous with a *cac*-lethal variant—exhibited defects in CPP, IPI, the pulse amplitude, and in the breadth of and number of peaks in the FFT-derived frequency spectrum (Table 1); but these flies were normal for *intra*-pulse frequency (a species-specific song character, *e.g.*, Bernstein *et al.* 1992). ANOVA revealed that significant differences existed between genotypes for each of these song parameters ($P < 0.001$). Post hoc comparisons of each genotype to both cac^+- and cac^S-expressing types revealed no significant differences from the control groups for intrapulse frequency or the two frequency spectrum parameters ($\alpha = 0.01$).

For both CPP and IPI song values, the *cac* genotypes fell into three groups: heteroallelic combinations of cac^S with lethal *cac* alleles or with the deletion were indistinguishable from mutant cac^S homozygotes; the $cac^S/+$ heterozygote was intermediate for these parameters; and the remainder of the genetic types were indistinguishable from wild type (Table 1; summary in Table 4). The CPP values form an essentially bimodal distribution, with a rather distinct break between mutant scores and ones that were like wild type, hence very few CPPs that could be termed intermediate. However, the IPIs computed from recordings of these many types led to a quasi-continuous distribution of interpulse intervals (as implied in Table 1), which is difficult to interpret. Nevertheless, the homozygous cac^{EE171}, cac^{H18}, and cac^{P73} types, heteroallelic combinations involving these three viable mutations, and combinations of these three mutations with the cac^- deletion, all gave CPP and IPI values that are almost certainly normal (Table 4). Flies carrying these mutations exhibited singing defects (with values intermediate between mutant-like and normal) only when a given mutation was heterozygous with certain lethal alleles (Table 4). Thus, we hypothesize that the particular Dmca1A changes in these lethals interact with the viable mutations in special ways to produce relatively subtle song problems that are not observed in flies carrying two doses of the visual mutations or one dose of them and no *cac* gene (*e.g.*, cac^{EE171}/Df).

For pulse amplitude, cac^S homozygotes and heteroallelic combinations with lethal *cac* alleles or the deletion (Df) gave mutant-like (high amplitude) scores, while $cac^S/+$ and $Df/+$ were intermediate. Although cac^{P73} homozygotes have normal amplitude values, the heteroallelic combination of cac^{P73} with cac^S led to high amplitudes. Combinations with the deletion and with several of the lethal alleles gave intermediate values, implying that the cac^{P73} mutant is hypomorphic for a function required for normal pulse amplitude. One problem with interpreting this result in the narrow sense is that these amplitude values are highly variable among genotypes, including some unusually large values at the high end of the mutant range. Nevertheless, other genotypic combinations involving cac^+, cac^{H18}, cac^{EE171}, and cac^{P73} (that is, except for cac^{P73}/cac^S and $cac^{P73}/lethal$) gave low song-pulse amplitudes in the normal range (whereby we take that range to be a value of *ca.* 13 or less; Table 1).

In summary, the cac^S mutation is overwhelmingly "the" song variant at the genetic locus encoding Dmca1A (see summary Table 4, below). Yet—to resist an impulse to view a given *cac* allele as exquisitely "specific"—we reiterate that one song anomaly was revealed in several genetic combinations involving the "visual-only" allele cac^{P73}. Analogous findings are included in the next three sections, meaning that we have teased out subtle visual defects in flies carrying the so-called "song-only" allele cac^S.

The *cac* mutants define a phenotypic series for visually mediated behaviors: *nbA* mutants exhibit certain subnormalities and anomalies in visual function, based on rather limited tests of visually-mediated behavior (see Introduction). We felt that a broader spectrum of visual tests should be applied to the full array of *cac*-locus variants, to better reveal which mutations are truly "visual-specific." The overall response of Drosophila to visual stimuli requires not only that photoreceptors function appropriately, but also that this signal be transmitted, integrated, and output to motor effectors; these behaviors constitute the basis for a global bioassay of these functions. We thus performed walking optomotor assays and a pair of phototaxis assays for all viable *cac* genotypic combinations and compared these results to

those from wild-type controls and from flies known to be blind (Table 2).

The optomotor assay measures the ability of flies to respond to moving visual cues in the environment. All combinations involving cac^{+}, cac^{S} or the lethal allele $cac^{L\text{-}24}$, which complements all visual phenotypes (see below) were normal in the optomotor assay (score >0.69, perfect score = 1.00). The heteroallelic combination $cac^{P73}/cac^{L\text{-}20}$ had an intermediate optomotor score (0.42). All other genotypes were optomotor-blind (<0.09) and in this sense behaved indistinguishably from the genetically blind or eyeless controls (Table 2; Table 4).

The countercurrent-phototaxis assay measures the effect of increasing light intensity on the ability of flies to phototax in a light gradient. cac^{EE171} homozygotes and heteroallelic combinations with lethal alleles (except $cac^{L\text{-}24}$), all of which were optomotor-blind, exhibited a robust response in this assay but with reversed sign (score <-0.44); that is, as light intensity increased, the flies' phototaxis scores were reduced to below those obtained in the dark, confirming Kulkarni and Hall (1987) for the phenotype of cac^{EE171}. The other genotypes fell into two distinct groups (Table 2): those indistinguishable from blind flies (score between -0.11 and 0.22), and those indistinguishable from wild type (score >0.41). Every optomotor-normal genotype was phototaxis-normal in the countercurrent-regression assay. In addition, cac^{H18} and cac^{P73} homozygotes, which were optomotor-blind, were phototaxis-normal in this assay.

The Y-tube phototaxis assay asks flies to choose between a dark tube and one illuminated at its distal end. The genotypes fell into four distinct groups (Table 2): those involving cac^{EE171} (except $cac^{EE171}/cac^{L\text{-}6}$, which gave a score not significantly different from the sightless controls) had negative scores (<-0.27); *cac* mutant types were indistinguishable from blind control flies (-0.13 and 0.09); two types yielded intermediate scores ($cac^{S}/cac^{L\text{-}6}$ and $cac^{P73}/cac^{L\text{-}6}$: 0.45 and 0.5); and a group of mutant types was indistinguishable from wild type (>0.69). Genotypes leading to nonblind countercurrent-regression scores gave similar results in this assay. The cac^{H18} heteroallelic combinations with either cac^{EE171} or cac^{P73} were phototaxis-blind in countercurrent-regression but normal in the Y-tube.

With the caveat that cac^{EE171} phototaxis scores are negative, the genotypes can be categorized as: behaviorally blind; Y-tube normal; countercurrent-regression- and Y-tube normal; or normal in all three assays (Table 2). This defines a gradient of defects in which relative severity of phenotypic consequence can be assigned (Table 4). The exceptions to this pattern are in the Y-tube assay and involve lethal allele $cac^{L\text{-}6}$. The behavior of $cac^{EE171}/cac^{L\text{-}6}$ is indistinguishable from blindness, and $cac^{S}/cac^{L\text{-}6}$ is intermediate between wild type and blind—although we predicted from the second data column of Table 2 that $cac^{EE171}/cac^{L\text{-}6}$ would be negatively phototactic and $cac^{S}/cac^{L\text{-}6}$ normally phototactic.

We uncovered special kinds of interactions between certain combinations of *cac*-locus variants—as opposed to a situation in which a given allele would always yield a certain phenotype whenever it is in combination with a *cac*-variant that falls within another particular category. Thus, for example, the cac^{P73} allele is optomotor-defective when homozygous or when combined with lethal *cac* alleles (except $cac^{L\text{-}24}$); and $cac^{L\text{-}20}$ is optomotor-defective with either cac^{EE171} or cac^{H18}, implying that both cac^{P73} and $cac^{L\text{-}20}$ have defects in functions required for normal optomotor behavior. However, the $cac^{P73}/cac^{L\text{-}20}$ combination is not optomotor-blind, although it does have a reduced optomotor score; this implies that these alleles might be defective in partially separable functions, such that each can complement the defect of the other. Another such example involves flies homozygous for cac^{H18} or cac^{P73}, which gave normal phototactic responses, and cac^{H18}/cac^{P73} flies, which were phototaxis-blind in the countercurrent-regression assay. Furthermore, the pattern of lethal alleles that uncovers blindness is different between these two viable alleles: The cac^{H18} phototaxis defect is uncovered by only three of the lethal alleles ($cac^{L\text{-}13}$, $cac^{L\text{-}6}$, and $cac^{L\text{-}20}$), while that of cac^{P73} is uncovered by an overlapping but different set of lethal alleles ($cac^{L\text{-}13}$ and $cac^{L\text{-}10}$). This suggests that cac^{H18} and cac^{P73} are hypomorphic for separable functions, such that two copies of either are sufficient to normalize the phenotype, but one copy of each is insufficient.

***cac* mutants have genetically separable ERG defects:** ERGs measure the summed light-induced electrical activity from photoreceptors and optic ganglia (*e.g.*, Pak 1975). We recorded ERGs from flies expressing all *cac*-associated genotypes and analyzed them for the presence and amplitude of lights-on and -off transients, as well as for the amplitude and kinetics of the LCRP (as defined in Figure 3A, Table 3). All genotypes involving cac^{+} or $cac^{L\text{-}24}$ led to quantitatively normal ERGs (Table 3), as did hemizygosity for cac^{S} (however, see next section for more on the latter mutant). Also, any *cac*-locus variant when heterozygous with cac^{+} resulted in normal ERGs (bottom of Table 3); this lack of dominant effects validates the mutant phenotypes observed in certain transheterozygotes.

ERGs from heteroallelic combinations involving cac^{H18}, cac^{EE171}, or cac^{P73} with each other or with lethal *cac* alleles (except $cac^{L\text{-}24}$) had no lights-on and -off transients. cac^{S} by itself has been thought to have no visual system defects (Kulkarni and Hall 1987; Homyk and Pye 1989). Yet, heteroallelic combinations of cac^{S} with cac^{H18}, cac^{EE171}, $cac^{L\text{-}6}$, $cac^{L\text{-}13}$, $cac^{L\text{-}20}$, or the cac^{-} deletion had lights-on transients that were significantly lower than normal in amplitude, and all of these genotypes except the combinations with cac^{EE171} and $cac^{L\text{-}20}$ led to low-amplitude lights-off transients (Table 3). The nominal significance of these amplitude reductions notwith-

TABLE 2

Visually mediated behaviors

Genotype	Walking optomotor score	Countercurrent phototaxis (×1000)	Y-Tube phototaxis score
norpA	−0.01 ± 0.02**	0.00 ± 0.07**	−0.01 ± 0.02**
eya[1]	−0.01 ± 0.02**	−0.01 ± 0.06**	−0.01 ± 0.02**
1/1	0.02 ± 0.11**	0.48 ± 0.17	0.78 ± 0.44
1/3	−0.11 ± 0.02**	−0.01 ± 0.09**	0.69 ± 0.02
1/4	0.09 ± 0.05**	−0.10 ± 0.06**	0.81 ± 0.02
3/3	0.06 ± 0.05**	−0.44 ± 0.07	−0.61 ± 0.03
3/4	−0.06 ± 0.09**	0.07 ± 0.88**	−0.08 ± 0.16**
4/−	−0.01 ± 0.07**	0.41 ± 0.26	0.85 ± 0.03
1/*Df*	0.00 ± 0.04**	0.00 ± 0.02**	0.05 ± 0.03**
1/*L-6*	−0.03 ± 0.08**	0.02 ± 0.09**	−0.05 ± 0.08**
1/*L-10*	0.03 ± 0.10**	0.66 ± 0.07	0.73 ± 0.01
1/*L-13*	−0.01 ± 0.03**	0.14 ± 0.09**	−0.13 ± 0.07**
1/*L-20*	0.04 ± 0.05**	0.03 ± 0.06**	0.09 ± 0.04**
1/*L-24*	0.87 ± 0.01	0.77 ± 0.13	0.83 ± 0.01
3/*Df*	0.01 ± 0.02**	−0.55 ± 0.13	−0.67 ± 0.04
3/*L-6*	0.02 ± 0.02**	−0.54 ± 0.03	− 0.13 ± 0.04**
3/*L-10*	−0.10 ± 0.07**	−0.64 ± 0.04	−0.27 ± 0.04
3/*L-13*	−0.10 ± 0.03**	−0.74 ± 0.03	−0.32 ± 0.01
3/*L-20*	−0.04 ± 0.07**	−0.62 ± 0.21	−0.29 ± 0.05
3/*L-24*	0.94 ± 0.02	0.62 ± 0.02	0.95 ± 0.01
4/*Df*	0.03 ± 0.03**	0.22 ± 0.17**	0.08 ± 0.04**
4/*L-6*	0.02 ± 0.04**	0.21 ± 0.12**	0.50 ± 0.09*
4/*L-10*	0.07 ± 0.08**	−0.11 ± 0.06**	0.03 ± 0.30**
4/*L-13*	−0.08 ± 0.04**	−0.04 ± 0.20**	−0.04 ± 0.16**
4/*L-20*	0.42 ± 0.09*	0.57 ± 0.18	0.96 ± 0.02
4/*L-24*	0.78 ± 0.02	0.54 ± 0.07	0.96 ± 0.01
cac/1	0.95 ± 0.02	0.73 ± 0.06	0.91 ± 0.03
cac/3	0.88 ± 0.07	0.44 ± 0.02	0.93 ± 0.02
cac/4	0.87 ± 0.07	0.75 ± 0.04	0.77 ± 0.02
cac/*cac*	0.96 ± 0.02	0.68 ± 0.04	0.96 ± 0.01
cac/*Df*	0.69 ± 0.08	0.54 ± 0.04	0.93 ± 0.01
cac/*L-6*	0.89 ± 0.03	1.09 ± 0.06	0.45 ± 0.04*
cac/*L-10*	0.93 ± 0.01	0.88 ± 0.12	0.71 ± 0.02
cac/*L-13*	0.91 ± 0.01	0.72 ± 0.06	0.85 ± 0.02
cac/*L-20*	0.83 ± 0.02	0.90 ± 0.07	0.82 ± 0.03
cac/*L-24*	0.94 ± 0.01	0.76 ± 0.08	0.87 ± 0.01
WT/1	0.94 ± 0.01	0.61 ± 0.08	0.84 ± 0.02
WT/3	0.96 ± 0.01	0.65 ± 0.06	0.91 ± 0.01
WT/4	0.94 ± 0.02	0.65 ± 0.05	0.91 ± 0.01
WT/*cac*	0.95 ± 0.02	0.75 ± 0.10	0.90 ± 0.01
WT/*Df*	0.78 ± 0.02	0.83 ± 0.09	0.82 ± 0.02
WT/*L-6*	0.92 ± 0.01	0.74 ± 0.07	0.90 ± 0.01
WT/*L-10*	0.95 ± 0.01	0.76 ± 0.09	0.89 ± 0.02
WT/*L-13*	0.93 ± 0.01	0.68 ± 0.08	0.91 ± 0.01
WT/*L-20*	0.92 ± 0.01	0.74 ± 0.10	0.90 ± 0.01
WT/*L-24*	0.96 ± 0.01	0.72 ± 0.08	0.94 ± 0.01
WT/WT	0.95 ± 0.00	0.66 ± 0.01	0.89 ± 0.01

no-receptor-potential-A (*norpA*^{P24}) and *eyes-absent* (*eya*[1]) are blind flies that are, respectively, phototransduction-deficient (no ERG, blind) and eyeless; all other genotypes are as in Table 1, with the additional case of "4/−", which designates *cac*^{P73}/Y males. Values are the mean of five independent experiments ± SEM. *cac*^{P73} homozygous females from the outcrossed stock rarely survived to adulthood, and those that did died within 1–2 days, so hemizygous *cac*^{P73} males were tested. Unmarked entries indicate values that are not significantly different from wild-type; **, values that are not significantly different from sightless controls; *, values that are significantly different from both blind flies and wild-type ($\alpha = 0.01$). Negative scores that are significantly different from sightless control flies are underlined. Supplementary nonparametric statistics showed genotypic distinctions the same as those determined from the other tests (except that *cac*/*Df* and *cac*/*L-20* were just subnormal). Nonparametric testing of countercurrent values came out the same as in the other tests (except that 4/4 was distinguishable from both wild-type and blind contols). Nonparametric and parametric test results for Y-tube phototaxis scores were congruent.

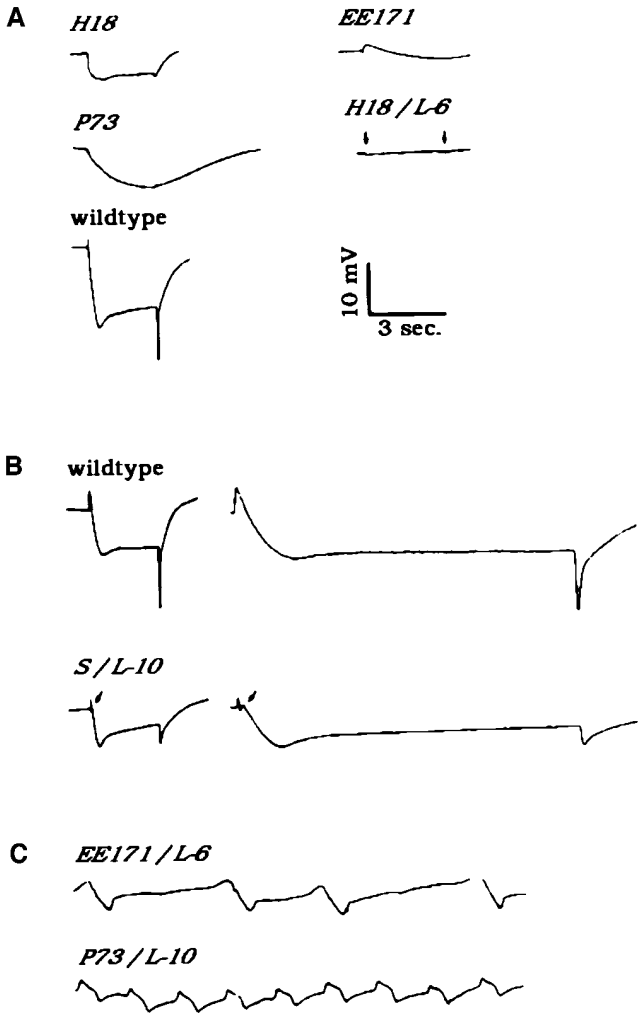

Figure 3.—Electroretinogram phenotypes of flies expressing various *cac* allelic combinations. Such alleles are indicated by superscripts only. ERGs were obtained by extracellular recordings from eyes of the indicated types; positive is up. Positive-going lights-on and negative lights-off transients (visible in "wild-type" traces in A and B) are caused by postsynaptic activity in the outer optic ganglia of the brain (Coombe 1986; Coombe and Heisenberg 1986; Pak 1975). The sustained negative light coincident receptor potential (LCRP) is caused by depolarization of photoreceptor cells, and in wild type typically has a quick (<1/2 second) overshoot phase, followed by a sustained phase. The "kinetic" measure of the LCRP (see text; Table 3) is the time interval between light-on and the maximum absolute amplitude of the LCRP; in the case of cac^{P73}, this corresponds to the time of lights-off. Downward-pointing arrows in the cac^{H18}/cac^{L-6} type indicate the time of lights on and off; this time can be inferred in other traces by the onset and offset of the LCRP or by the onset and offset of transients; the interval between lights-on and -off is three seconds in all cases. (A) ERGs from wild-type and representative of those from the indicated *cac* mutants. (B) Representative examples of ERGs expressing a novel rebound component of the ERG; the second trace of each is expanded 5× in time. (C) Representative examples of ERGs expressing a novel light-refractory, wandering-baseline phenotype.

standing (Table 3), we point out that the ERG transients measured in flies expressing the cac^S combinations (for example) were approximately 60% of normal, *i.e.*, amplitude values from cac^+-bearing controls or other types, such as cac^S/cac^S, that gave control-like values.

We found that several *cac* mutants have distinctive and easily recognizable LCRP aberrations (Figure 3; Table 3): cac^{H18} had a normal-appearing LCRP with significantly reduced amplitude; cac^{EE171} a low-amplitude LCRP with an initial reversal of polarity; and cac^{P73} a low-amplitude LCRP with slow kinetics of onset and recovery (Figure 3A). Heteroallelic combinations of cac^{H18}, cac^{EE171}, or cac^{P73} each produced LCRPs that fit one of these categories. The cac^{H18} LCRP-shape phenotype is dominant to cac^{EE171} and cac^{P73} alleles, and cac^{EE171} is dominant to cac^{P73}. With one exception, heteroallelic combinations with the lethal *cac* alleles (except cac^{L-24}) uncovered the LCRP shape associated with the relevant viable *cac* allele: cac^{P73}/cac^{L-13} has a cac^{EE171}-like LCRP shape. Also, the cac^{P73}/cac^{L-6} type gave a normal LCRP amplitude but defective kinetics, while cac^{H18}/cac^{P73} exhibited a defective LCRP but normal kinetics. Thus, these two ERG components are separable.

We discovered an additional special kind of interaction involving the lethal mutation cac^{L-6} (*cf.* previous section). Although cac^{P73} hemizygotes had normal LCRP amplitudes, the cac^{P73} heteroallelic combinations with cac^{H18}, cac^{EE171}, or with most lethal alleles had low amplitudes; this implies that cac^{P73} is hypomorphic for this phenotype and unable to complement the amplitude defect of these alleles. The cac^{L-6} heteroallelic combinations with cac^{H18} and cac^{EE171} nearly abolished the LCRP (Table 3), even though cac^{H18} and cac^{EE171} homozygotes and heteroallelic combinations with other lethal alleles or the deletion had intact LCRPs (albeit of reduced amplitude). However, the cac^{P73}/cac^{L-6} type showed a normal LCRP amplitude. The cac^{L-6} allele must retain a function for which cac^{P73} is hypomorphic but would seem to be damaged in a (separate) function in which cac^{H18} and cac^{EE171} are defective.

In summary, the *nbA* mutations at this locus (by themselves, or when placed over most of the lethal alleles) lead to blatant ERG defects (Table 4). Combinations involving cac^S and two of the *nbA*s did produce smaller than normal transient spikes (Table 4). But this mild abnormality should not be taken to infer an all-out lack of complementation, especially inasmuch as other visual parameters are normal or close to it in these transheterozygotes (cac^S/nbs^{H18} or cac^S/nbA^{EE1}) and other heteroallelic combinations involving cac^S and several of the genetic variations at the locus (Table 4). Conservatively, however, it is once again not warranted to claim that viable *cac*-locus mutants are completely without pleiotropies—by virtue of causing song defects and no visual ones at all, or vice versa. The next section includes some further suggestions that the so-called song mutation

TABLE 3

Electroretinograms

Genotype	*n*	Rebound or refract	On transient (mV)	LCRP amplitude (mV)	Time to max. amplitude (sec)	Off transient (mV)
1/1	4	rbnd-1	N/P	4.8 ± 0.5**	0.40 ± 0.09	N/P
1/3	4		N/P	6.0 ± 0.7**	1.40 ± 0.19**	N/P
1/4	4		N/P	3.5 ± 0.3**	0.40 ± 0.07	N/P
3/3	4		N/P	4.3 ± 0.3**	2.78 ± 0.13**	N/P
3/4	4	2::6	N/P	4.5 ± 1.3**	2.95 ± 0.05**	N/P
4/−	4	rbnd	N/P	10.3 ± 0.9	2.83 ± 0.12**	N/P
1/*Df*	4		N/P	2.6 ± 0.2**	0.30 ± 0.07	N/P
1/*L-6*	4		N/P	WEAK N/A	N/A	N/P
1/*L-10*	4		N/P	2.5 ± 0.3**	0.45 ± 0.09	N/P
1/*L-13*	4		N/P	3.1 ± 0.5**	0.33 ± 0.08	N/P
1/*L-20*	4		N/P	2.4 ± 0.2**	0.38 ± 0.03	N/P
1/*L-24*	4		2.3 ± 0.1	10.5 ± 0.6	0.45 ± 0.03	4.38 ± 0.19
3/*Df*	4	5::9	N/P	3.0 ± 0.4**	2.85 ± 0.10**	N/P
3/*L-6*	3	7::10	N/P	WEAK N/A	N/A	N/P
3/*L-10*	4	4::8	N/P	2.8 ± 0.5**	2.90 ± 0.10**	N/P
3/*L-13*	4	6::10	N/P	4.6 ± 1.3**	2.85 ± 0.10**	N/P
3/*L-20*	4	6::10	N/P	4.6 ± 0.6**	2.90 ± 0.10**	N/P
3/*L-24*	4		3.3 ± 0.5	12.5 ± 0.9	0.53 ± 0.03	3.80 ± 0.42
4/*Df*	4	4::8	N/P	3.0 ± 0.7**	2.90 ± 0.06**	N/P
4/*L-6*	4	5::9	N/P	13.0 ± 0.7	3.00 ± 0.00**	N/P
4/*L-10*	3	6::9	N/P	2.3 ± 0.9**	1.83 ± 0.06**	N/P
4/*L-13*	3	6::9	N/P	2.0 ± 0.6**	2.47 ± 0.07**	N/P
4/*L-20*	4	5::9	N/P	4.3 ± 0.9**	1.60 ± 0.18**	N/P
4/*L-24*	4		2.5 ± 0.2	12.3 ± 1.9	0.53 ± 0.03	4.00 ± 0.37
cac/1	4	rbnd-2	1.8 ± 0.2**	11.8 ± 0.5	0.40 ± 0.00	3.10 ± 0.44**
cac/3	4		1.8 ± 0.1**	16.8 ± 0.9	0.40 ± 0.00	4.90 ± 0.19
cac/4	4	rbnd-1	2.2 ± 0.3	14.3 ± 0.9	0.40 ± 0.04	3.75 ± 0.36
cac/*cac*	4		2.8 ± 0.3	14.5 ± 0.6	0.40 ± 0.04	6.20 ± 0.50
cac/*Df*	4	rbnd	1.6 ± 0.2**	14.5 ± 0.6	0.53 ± 0.03	2.40 ± 0.16**
cac/*L-6*	6	rbnd	1.7 ± 0.2**	8.5 ± 0.4	0.52 ± 0.04	2.10 ± 0.44**
cac/*L-10*	4	rbnd	3.1 ± 0.3	12.3 ± 1.3	0.50 ± 0.00	3.80 ± 0.74
cac/*L-13*	4	rbnd	1.7 ± 0.2**	16.0 ± 0.8	0.50 ± 0.00	3.10 ± 0.25**
cac/*L-20*	4	rbnd	1.5 ± 0.2**	14.5 ± 0.3	0.40 ± 0.00	3.70 ± 0.34
cac/*L-24*	4		2.5 ± 0.2	14.0 ± 0.7	0.45 ± 0.03	5.20 ± 0.16
WT/1	4		2.9 ± 0.3	11.3 ± 1.1	0.53 ± 0.03	4.40 ± 0.43
WT/3	4		2.1 ± 0.1	10.8 ± 0.9	0.43 ± 0.03	2.80 ± 0.93
WT/4	4		2.4 ± 0.1	10.3 ± 0.5	0.48 ± 0.03	5.00 ± 0.42
WT/*cac*	4		3.6 ± 0.5	12.8 ± 1.0	0.48 ± 0.03	4.00 ± 0.67
WT/*Df*	4		3.4 ± 0.2	11.8 ± 1.3	0.45 ± 0.03	4.70 ± 0.34
WT/*L-6*	4		2.6 ± 0.2	8.9 ± 0.4	0.43 ± 0.03	4.60 ± 0.35
WT/*L-10*	4		2.6 ± 0.4	14.0 ± 0.9	0.40 ± 0.00	5.70 ± 0.38
WT/*L-13*	4		2.6 ± 0.2	11.3 ± 0.5	0.43 ± 0.03	3.80 ± 0.35
WT/*L-20*	4		2.1 ± 0.3	13.5 ± 1.0	0.40 ± 0.04	3.30 ± 0.19
WT/*L-24*	4		2.6 ± 0.3	11.0 ± 1.1	0.43 ± 0.03	5.05 ± 0.34
WT/WT	6		3.1 ± 0.3	11.8 ± 0.6	0.43 ± 0.02	4.93 ± 0.50
OR-R	10		2.8 ± 1.5	12.3 ± 0.4	0.48 ± 0.02	5.70 ± 0.38

Genotypes are as in Table 2, with the addition that "OR-R" designates an Oregon-R strain, males from which were used as an extra wild-type control. N/P, the relevant transient is not present in that genotype; WEAK, the LCRP is visually detectable in records from the indicated genotype, but not measurable. All values are means ± SEM. **, values that are significantly different from wild type; *, values that are not significantly different from wild type ($\alpha = 0.01$). Ratios (double colons) represent the number of flies having a light-refractory wandering-baseline phoenotye (see text and Figure 3C) out of the total number of flies examined; the remaining flies did not exhibit this character and represent the number of flies (*n*) examined for ERG phenotype. "rbnd", the presence of an aberrant rebound waveform phenotype similar to that in Figure 3B; those entries with a number following a hyphen represent the number of flies of that genotype that exhibited the rebound phenotype.

TABLE 4

Summary of courtship-song and visual-response phenotypes

Geno-type	Song	Optomotor	CC-photaxis	Y-photaxis	Transients	LCRP amplitude	LCRP kinetics	Rebound	Refractory wandering
cac $^{H18=1}$	+	−	− (+1, *L-10*)	− (+1, 3, 4, *L-10*)	−	− (weak, *L-6*)	+ (−3)	±	+
cac $^{EE171=3}$	+	−	neg. (−1, 4)	neg. (+1; −4,*L-6*)	−	− (weak, *L-6*)	−	+	−
cac $^{P73=4}$	+ (±Amp)	− (±*L-20*)	− (+4, *L-20*)	− (+1, 3, 4, *L-20*, ±*L-6*)	−	− (+4, *L-6*)	− (+1)	−	−
cac ^{S}	−	+	+	+	±	+	+	−	+
Df	−	−	−	−	−	−	−	−	−
L-6	−	−	−	− (−3*; ±4)	−	± (−1, 3; +4)	−	−	−
L-10	−	−	− (+1)	− (+1)	−	−	−	−	−
L-13	−	−	−	−	−	−	−	−	−
L-20	−	− (±4)	− (+4)	− (+4)	−	−	−	−	−
L-24	−	+	+	+	+	+	+	+	+

cacophony genotypes are designated in the lefthand column. These include shorthand indicators, whereby visually related alleles at the *cac* locus are named according to the dicta of Lindsley and Zimm (1992); hence 1 = *cac* ^{H18}, 3 = *cac* ^{EE171}, and 4 = *cac* ^{P73}; *Df* is a small *X*-chromosomal deletion [called *Df(1)RC29*] that removes the *cac* locus and a few neighboring ones, the *L*s are lethal genetic changes at the *cac* locus (alone). The many possible combinations involving viable *cac* alleles (including the *cac* $^{+}$ control one) and the *cac* $^{-}$ (or otherwise *cac*-lethal) ones are compressed as follows: First four rows: viable mutations homozygous with themselves or hemizygous with a *Y* chromosome in a male. Next row: the *cac* $^{-}$ *Df*, heterozygous with *cac* ^{S} for the first data column, or with the visual mutations (1, 3, or 4) for the remaining such columns. Last five rows: a given *cac*-lethal (*L*) mutation, again, heterozygous with *cac* ^{S} for song recordings or over the other (numbered) *cac*-viables for tests of visual-system function. "Song" (first data column) refers in particular to abnormalities (or the lack thereof) of interpulse intervals, cycles per pulse, and pulse amplitudes (see Table 1). The next three columns refer to visually mediated adult behaviors, measured in walking optomotor tests, and those involving counter-current phototaxis and Y-maze phototaxis (see Table 2). The last five columns stemmed from electroretinogram (ERG) recordings (see Table 3): the presence (including measurements) of light-on and light-off transient spikes; amplitudes of light-coincident receptor potential; the kinetics of LCRP onset; a "rebound" voltage change occurring in conjunction with the light-on transient (see Figure 3B); and anomalous light-refractory/wandering baseline voltage changes (see Figure 3C).

General rules for phenotypes of heterozygotes: *cac* ^{S} over 1, 3, or 4, normal song and vision; *cac* ^{S} over *L*'s, mutant song and normal vision (except for ERG "rebound"); 1, 3, or 4 over *L*'s, normal song and mutant vision (except for *L-24*: normal vision). +, effects of the *cac*-locus variant in the row or genetic combinations involving it and other such variants were normal for the phenotype in the column; −, for viable alleles (first four rows), the mutant is mutant for the phenotype in the relevant column, or genetic combinations involving lethal variants (bottom six rows) and others at the locus are mutant for the relevant phenotype; ±, the relevant mutant, or genetic combination involving a lethal variant and a viable one, gave intermediate scores, or a subset of the transheterozygotes (*e.g.*, involving an *L* or lethal variant and certain viable mutations) yielded a mutant phenotype; neg, negative phototaxis (anomalous); parentheses, exceptions to the general phenogenetic rules, *e.g.*, the song-pulse amplitude for *cac* ^{P73} was intermediate between normal and *cac* ^{S}-like, but other song parameters were normal.

causes additional problems with visual-system functioning.

Novel ERG phenotypes of *cac* mutants: In flies expressing several of the *cac*-variant genotypes, we observed a low-amplitude rebound component superimposed on the transition between the lights-on transient and the LCRP (Figure 3B; Table 3). Such an "extra" component seemed to us to be more pronounced than the subtle complexities that can accompany the electrical signals recorded (from Drosophila's visual system) when the lights go on or off (Heisenberg 1971). Moreover, what we judge to be a rebound abnormality was seen only in certain genotypes: heteroallelic combinations of cac^{S} with vision-defective lethal alleles, with the deletion, or with cac^{H18} and cac^{P73}, and also in cac^{H18} and cac^{P73} homozygotes; however, it was not seen in cac^{S} homozygotes (Table 4). A similar but much subtler break in the ERG trace was sometimes seen in cac^{P73} heteroallelic combinations with lethal *cac* alleles, but the discontinuity was of much lower amplitude and not reliably scorable. The peak of the rebound component (Figure 3B) is temporally aligned with the peak of the corneal-positive component in cac^{EE171} ERGs, implying that these might have a similar etiology. The appearance of a rebound component in some ERGs from cac^{H18} and cac^{P73} homozygotes, in which the transients are entirely missing, implies that this phenotype is separable from the lights-on transient defects.

An additional, novel ERG phenotype was sometimes observed in several cac^{EE171}/cac^{P73} heterozygotes and in heteroallelic combinations of these with vision-defective lethal alleles (Table 4). These flies' visual systems produced a distinctive cyclic wandering of the baseline ERG potential, independent of any specific light stimulus (Figure 3C). The amplitude was variable but in no case exceeded the amplitude of normal LCRPs. In addition, these flies were refractory to light-induced responses, in that there was no apparent change in extracellular potential in response to specific light stimulation. Individual flies with detectable light-coincident responses were never observed to exhibit this cyclic wandering of the baseline ERG potential. Moreover, this baseline wandering/light-refractory phenotype was never observed in recordings from other mutant genotypes reported here or in over 250 recordings from wild-type control animals. These additional facts (that is, aside from the mutant result exemplified in Figure 3C) lead us to suggest that the wandering baseline phenotype is not an artifact (such as background noise, signals picked up from the brain, muscles, or heart, or unwanted movements of the specimen).

Genotypes involving $cac^{L\text{-}24}$ (which is also intact for all other visual functions assayed) did not exhibit either of these novel ERG phenotypes ("rebound," "wandering baseline"; Table 4). Flies expressing cac^{H18} or cac^{S} did not exhibit the wandering/refractory phenotype; and genotypes involving cac^{EE171} did not cause the rebound

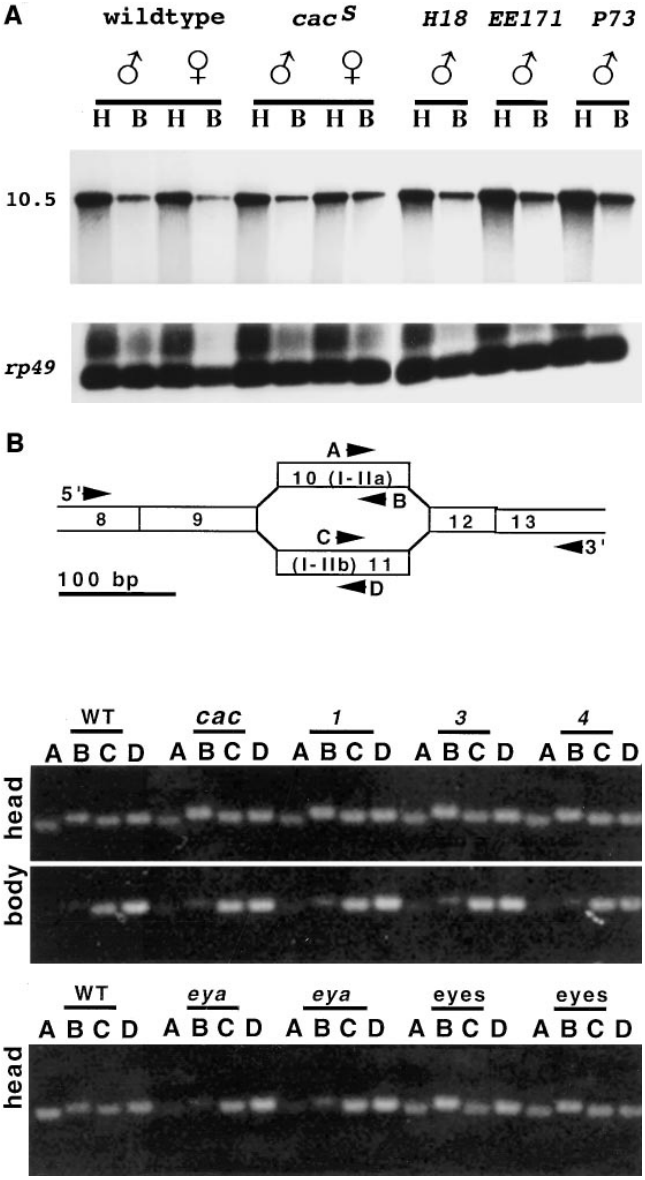

Figure 4.—Expression of Dmca1A transcripts. (A) Northern blots of head and body RNA from wild-type and mutant adult flies, detected with a Dmca1A-specific probe (see Figure 1). (B) Tissue-specific expression of exons I-IIa and I-IIb. The diagram shows the organization of the Dmca1A transcript and the relative positions (arrowheads) of primers used for isoform-specific semiquantitative RT-PCR. Agarose gels of RT-PCRs were ethidium-stained and photographed. The top lines of headers for the gels indicate (in the main) genotypes of the flies from which the head or body RNAs were extracted: WT, wild-type; *cac*, the song mutant cac^{S}; 1, 3, and 4 the visual mutants cac^{H18}, cac^{EE171}, and cac^{P73}; *eya*, *eyes-absent*; "eyes," RNA was extracted only from that WT tissue. Below the genotype or tissue-type headers are designations for the exon-specific primers used, *i.e.*, A, B, C, or D. In this semiquantitative analysis, the amplification levels of the four PCR products are not comparable with each other, but amplification levels of each product within an experiment are comparable between individuals (see text).

phenotype, indicating that these visual defects are genetically separable from each other.

Dmca1A transcripts in *cac* mutants: We analyzed mRNAs transcribed from the *cac* gene to ask whether there is a molecular corollary to the "vision-specific" mutations at this locus. Northern-blot analyses indicated, first of all, that the Dmca1A transcript is enriched in heads compared to bodies, and that there were no differences in Dmca1A transcript expression levels between males and females from a wild-type strain or from one carrying the cac^S mutation (Figure 4A). None of the viable *cac* mutations caused any substantial expression level or transcript size abnormality of the Dmca1A transcript in either body or head.

Given that the vision-defective cac^{H18} mutant has a stop codon in exon I/IIa, we asked if transcripts containing either exon I/IIa or I/IIb were expressed in the eye or in other tissues. We designed 5′ and 3′ PCR primers internal to these exons and used these with primers specific to flanking exons to amplify 188–250-bp RT-PCR products from cDNA derived from body, head, or eyes of adult wild-type, *cac*, and *eyes absent* (eya^1) mutant flies (Figure 4B). Each of these four primer pairs yielded a product of the expected size. Southern blotting and hybridization with a Dmca1A probe, and lack of a detectable product in non-reverse-transcribed control reactions, confirmed that the products are specifically amplified from Dmca1A transcripts. Sequence analysis of a representative of each product and detection of the cac^{H18} mutation in the appropriate product further confirmed the specificity of the RT-PCR products (data not shown). Amplification of a specific RT-PCR product using two different primer pairs for each of these exons, for each of the mutants, demonstrated that both exons I/IIa and I/IIb are expressed in heads, bodies, and eyes of wild-type and each of the viable *cac* mutant flies.

To allow semiquantitative analysis of differences in transcript expression levels, we used input quantities of cDNA that were subsaturating for our PCR conditions (Huet *et al.* 1993; see materials and methods). Each of the four RT-PCR products (A, B, C, D; Figure 4) are from different primers, amplify different sequences, and use different input quantities of cDNA, so apparent quantitative differences between the four different RT-PCR products do not directly reflect underlying quantitative differences in RNA levels. However, the *ratio* of amplification of each product relative to the others is reproducibly consistent between experiments. In Figure 4B, note the pattern of amplification levels of A and B (specific to exon I/IIa) and C and D (specific to exon I/IIb) and, within a given tissue, the invariant nature of that pattern between wild-type and *cac*-mutant types. These data indicate that none of the mutants has any substantial effect on the relative expression levels of exons I/IIa and I/IIb.

Amplification from primer pairs A and B relative to C and D is reduced in body compared to head RNA, indicating that the proportion of transcripts containing exon I/IIa is likely to be relatively lower in body than in head. Similarly, reduced amplification from primer pairs A and B from eya^1 heads, which have no compound eyes, indicates that exon I/IIa expression is relatively low in these heads and therefore likely to be high in the eye. This was confirmed by analysis of RNA from isolated eyes, in which the relative amplification of exon I/IIa-specific products was similar to that in intact heads. This semiquantitative analysis gave no indication of the absolute levels of each transcript or of the absolute levels of the differences between them. However, the clear and reproducible differences in relative amplification levels of exon I/IIa- and I/IIb-derived RT-PCR products confirms that transcripts containing each exon are present in eyes, in heads, and in bodies and implies that expression of exon I/IIa is relatively enriched in the eye. These RNA-based results seems very likely to be related to the findings (presented above) about the apparent elimination of the I/IIa Dmca1A isoform by a *cac-nbA* mutation (Figures 2 and 3) which leads exclusively to visual defects (Table 4).

DISCUSSION

The *cac* gene encodes the Dmca1A calcium-channel α1 subunit: Phenogenetic analysis reveals that *cac* specifies an essential gene product that is involved in the operation of the visual system (*cf.* Pak 1975; Zuker 1996) and thoracic neuromuscular systems (*cf.* Hall *et al.* 1990; Hall 1994) as well as being required for specific behavioral and physiological functions. The Dmca1A transcription unit maps to *l(1)L13*-associated chromosomal lesions (Kulkarni and Hall 1987; Smith *et al.* 1996), and the cac^S and cac^{H18} mutants have sequence polymorphisms that cause significant changes in the predicted Dmca1A protein.

It is still conceivable that this *nbA* (*H18*) mutation and the *cac* one (*S*) define two different functions (or even genes); but the fact that both are mutated in the same ORF, which encodes a protein that can be considered highly relevant to both song-ralated and visual-system functions (see below), increases the weight of evidence in favor of these two different kinds of mutants having identified the same molecular-genetic entity. Furthermore, the phenotypic interrelatedness of *cac* and *nbA*-defined functions has been boosted by elements of the current results. Thus, several genetic combinations involving cac^{P73} (originally isolated on the basis of visual defects) give reduced courtship-song pulse amplitude, and several genotypes involving the cac^S mutation (identified initially with respect to an anomalous courtship song) have subtle ERG defects. The coupling of courtship-song and visual phenotypes, previously thought to be strictly separated between mutually exclusive classes of these interacting mutants, further suggests that all these mutations are allelic. We conclude that the *cac*

gene encodes the Dmca1A calcium channel α1 subunit protein, that this protein is an important factor mediating behaviorally-related functions of excitable cells, and that mutations in this gene are responsible for the various phenotypes of *cac* mutants.

Calcium-channel function in the generation of courtship song: The cac^S mutation does not lead to pathological abnormalities in the courtship song, but causes quantitative changes in elements of the song (Kulkarni and Hall 1987; Wheeler *et al.* 1989), leaving these acoustical signals nicely patterned. The cac^S mutation causes analogous (meaning nonpathological) changes in visual system physiology: it reduces the amplitude of the ERG transients (but does not eliminate them) and causes a novel but low amplitude aberration in the ERG. Also, the $cac^S/cac^{L\text{-}6}$ heteroallelic combination has defective Y-tube phototaxis. The cac^S mutation is in Dmca1A exon 19; this exon seems not to be subject to alternative splicing (Peixoto *et al.* 1997), so it would be expected to be included in all products expressed from the *cac* locus. These results imply that the cac^S mutation damages Dmca1A channel functions common to physiological processes underlying the generation of courtship song (Figure 5) and of a normal ERG, but not sufficiently (except in the one case just noted) to disrupt visually-mediated behaviors.

Mutations in ion-channel genes have often been associated with temperature-sensitive phenotypes such as paralysis (*e.g.*, Wu and Ganetzky 1992; Ganetzky 1996). In this context, an additional *cacophony* phenotype, temperature-sensitive convulsions, was recently discovered to be a feature of the "song allele" cac^S but not the "vision alleles" cac^{H18} and cac^{EE171} (Peixoto and Hall 1998). This raised the question of whether other temperature-sensitive ion-channel mutants would sing abnormally. Indeed, mutations at the *slowpoke* (*slo*) locus in *D. melanogaster*, which encodes a calcium-activated potassium channel (Atkinson *et al.* 1991) cause severe song defects (Peixoto and Hall 1998). Calcium and potassium currents are involved in the function of pacemaker cells (Hille 1992). Figure 5 presents a simple, speculative scheme of how the products of *cac* and *slo* could work together to form a pacemaker that would underlie the tone-pulse component of Drosophila's courtship song.

The lovesongs of these flies are thought to be involved in species recognition as well as stimulation of females to copulate and hence are hypothesized to be a component of prezygotic isolation during speciation (Coyne 1992; Hall 1994). It is intriguing that changes in courtship song caused by the cac^S mutation—specifically affecting the number of cycles per pulse, the interpulse interval, and the pulse amplitude (Figure 5)—are similar to the differences in song between several closely related species. The quasi-separability of *cac* phenotypes implies that it might be possible to "tune" the courtship song with relatively small evolutionary changes in this one gene. It will be interesting to examine the homologous channel protein from species known to differ in their song components (reviewed in Hall 1994) for differences that might contribute to evolutionary divergences of these species signatures. A gene such as *slo* may harbor song-related interspecific variations as well.

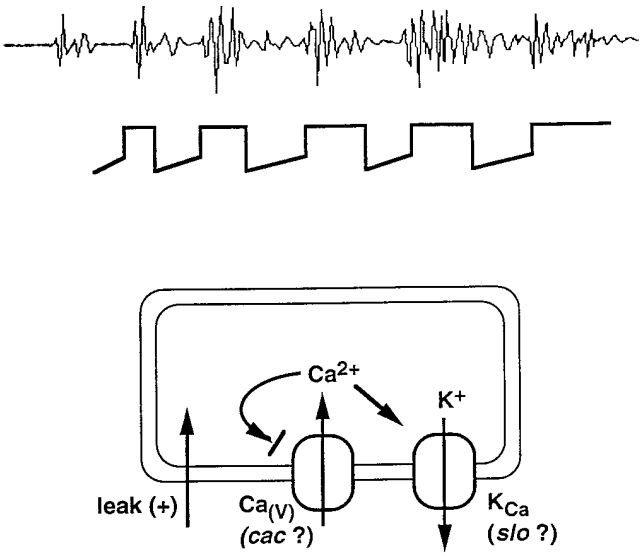

Figure 5.—How the *cacophony*-encoded calcium-channel subunit could exert a key feature of courtship-song control. At the top, part of a train of song pulses is shown (occurring over about 0.25 sec) above a crude indication of voltage changes that accompany the function of a generic pacemaker cell (*cf.* Hille 1992); six tone pulses—recorded from a diplo-*X* cac^S/cac^S fly transformed into a male by homozygosity for the *tra* mutation—are shown (thus, five interpulse intervals, whose timespans are ca. 40–45 msec); as is typified by this mutant's song, only the first two pulses exhibit cycle numbers in the normal range, with the others being abnormally polycyclic; the sawtooths below the song trace represent a hypothetical alignment of cyclic membrane potential changes in a song-controlling pacemaker cell with the repetitive bursts of courtship-song pulses; depolarized states, coinciding with the pulses, are caused by processes outlined in the bottom part of the figure: Here, a "leak" current in "bursting" cells causes a slow depolarization, eventually reaching a threshold and triggering a burst of action potentials (*cf.* Hille 1992); this causes Ca^{2+} entry through voltage-dependent Ca^{2+}-channels (whose α subunits are suggested to be encoded by *cac*); this in turn activates $K_{(Ca)}$ channels (suggested to be encoded by the *slo* gene—mutant forms of which cause song disruptions; see text); this causes Ca^{2+}-dependent inactivation of Ca^{2+} channels, which in turn leads to eventual hyperpolarization and cessation of action potentials; membrane potential and intracellular calcium return to basal levels, and the cycle can start again (*cf.* Hille 1992).

A phenylalanine (analogous to the cac^S-mutated residue) in the transmembrane domain of the minK subunit of the I_{sK} potassium channel (Wang *et al.* 1996) has been subjected to *in vitro* mutagenesis (Wilson *et al.* 1994). This protein change (F to C at residue 57) led to an I_{sK} potassium current that was normal in terms of half-maximal activation voltage and effect on membrane potential; that is, indistinguishable in these pa-

rameters from I_{sK} currents stemming from the expression of molecularly unaltered transcripts. However, the evolutionary and structural divergence of the minK protein makes it difficult to extrapolate these results to the Dmca1A calcium channel. Our results draw attention to the role of this transmembrane region (IIIS6)—and in particular to the *cac*-defined phenylalanine within it, which is now accessible for electrophysiological bioassay via analysis of calcium currents in cac^{S} mutant flies—in the function of calcium channels in general.

Dmca1A channel function in the visual system: The cac^{H18} mutant has defects in most visual phenotypes assayed but no defects in courtship song, and it carries a mutation that creates a stop codon within the alternative exon I/IIa, indicating that Dmca1A isoforms containing at least this variant motif are necessary for and specific to normal visual function. (Recall that "variant" means this exon encodes a stretch of amino acids that is hypothesized not to be able to interact with the typical β subunit.)

What might be the specific etiology of the vision defects in *cac* mutants? The mutations could cause developmental or degenerative defects in the optic ganglia or in retinula cells; indeed, degeneration has been reported for many mutations that affect visual transduction (Ranganathan *et al.* 1995). We confirmed the presence of a deep pseudopupil, an indicator of intact eye structure, during preparation for ERG recording in all genotypes tested (not shown). However, we cannot rule out a subtle morphological or degenerative defect in the genotypes examined in this report.

The absence or reduced amplitude of ERG transients in *cac* mutants, even in genotypes with robust (if aberrant) LCRPs, indicates a probable defect in transmission from the retinula cells to postsynaptic cells in the lamina (*cf.* Pak 1975). Synaptic neurotransmitter secretion is known to be dependent on calcium influx mediated by voltage-dependent calcium channels (reviewed by Dunlap *et al.* 1995). While the defect in transmission could be pre- or postsynaptic, an attractive hypothesis is that a class of synapse-specific Dmca1A channel isoforms is affected by these mutations.

That the LCRP in the most severely affected *cac* mutants is almost completely eliminated implies that such a genotype (visual mutation heterozygous with a lethal) causes an almost total failure of photoreceptor excitation—with the proviso that an increased stimulus intensity might have coaxed a small degree of depolarization from these mutant types. In Drosophila and other invertebrates, photoexcitation of rhodopsin molecules leads to G-protein-mediated activation of phospholipase-C and generation of inositol phosphates (reviewed by Ranganathan *et al.* 1995; Zuker 1996), followed by a light-activated inward current carried predominantly by Ca^{2+} and thought to be mediated by cation channels formed by the transient receptor potential (TRP) and TRP-like (TRPL) proteins (Niemeyer *et al.* 1996; and see Clapham 1996, for other-organismic connections). Ca^{2+}-CaM-regulated Ca^{2+} release from ryanodine-sensitive stores is believed to be involved in generation of the light-activated current (Phillips *et al.* 1992; Hardie and Minke 1993; Hardie 1996; Arnon *et al.* 1997). Inactivation of phototransduction appears to require an influx of extracellular Ca^{2+}, hypothetically involving calcium-regulated phosphorylation mechanisms (Kahn and Matsumoto 1997). Adaptation, or variation of the gain of phototransduction in varying light levels, is controlled by light-dependent changes in intracellular calcium levels, likely mediated by an eye-specific protein kinase C encoded by the *inaC* gene (Ranganathan *et al.* 1995). Given the regulatory role of calcium in phototransduction, it seems that aberrant calcium regulation due to defective Dmca1A calcium channel function could disrupt phototransduction. Indeed, the ERG of *trp* mutants exhibit a transient near-normal LCRP followed by a rapid decay, and intense light stimulation has been shown to completely but reversibly inactivate *trp*-mutant photoreceptors; these phenotypes have been suggested to be due to exhaustion of intracellular Ca^{2+} stores secondary to the defect in TRP-mediated calcium influx (Minke *et al.* 1975; Minke 1982). Regardless of etiology, it is clear that defects in proteins involved in calcium influx can have profound effects on phototransduction.

Voltage-activated Dmca1A-encoded calcium currents should now be considered a candidate to contribute under physiological conditions to the predominantly calcium-mediated light-activated current—subsequent to the light-dependent initiation of retinula depolarization, which is mediated by TRP and TRPL currents. Our current phenogenetic and molecular results suggest that further experiments—in particular, the analysis of Dmca1A and other ion currents in photoreceptors of *cac*-mutant flies—could decipher the contributions of Dmca1A calcium currents to membrane excitability or calcium regulation of phototransduction.

Phenotypic interactions and separability of *cac*-encoded functions: The multiple phenotypes, complicated genetic interactions, and extensive intragenic complementation imply that *cac* mutations affect Dmca1A channel functions that are at least partially separable (Table 4). Consideration of complementation patterns between viable and lethal *cac* alleles supports this idea. A deletion that removes the *cac* locus failed to complement all viable alleles for all phenotypes assayed. The $cac^{L\text{-}6}$ allele has allele-specific effects on LCRP amplitude, in that it dramatically worsened the amplitude defect of cac^{H18} and cac^{EE171} but complemented the amplitude defect of cac^{P73}. The $cac^{L\text{-}6}$ allele also partially complements the Y-tube phototaxis defect of cac^{P73}, and its heteroallelic combination with cac^{EE171} caused blindness in the Y-tube phototaxis assay rather than negative phototaxis. The $cac^{L\text{-}10}$ allele complements cac^{H18} for phototaxis only. The effects of the $cac^{L\text{-}13}$ allele are identical to those of the deletion, indicating that $cac^{L\text{-}13}$ is null for all functions assayed. The $cac^{L\text{-}20}$ allele partially complements cac^{P73} for optomotor behavior and

fully complements cac^{P73} in both phototaxis assays. The cac^{L24} allele complements every visual phenotype, but not courtship song.

The ensemble of our phenogenetic analyses (as summarized in Table 4) indicates that (1) cac^{H18} and cac^{P73} are hypomorphic for phototaxis, in that homozygotes with two copies of the mutant gene give normal behavior, but one copy of either (when heteroallelic with the deletion) reveals a mutant phenotype; (2) only one of these lethal *cac* alleles (cac^{L13}) is null, in that the others each complement *cac* phenotypes that the deletion does not; (3) the lethal *cac* alleles (except cac^{L13}) must each have different, putatively separable undamaged functions, in that they each are able to complement (and therefore retain functions required for) different subsets of phenotypes and of the viable *cac* alleles; and, as a corollary, (4) the viable *cac* alleles must have different separable damaged functions, in that they each exhibit a different pattern of complementation by the several lethal alleles.

Other results also reveal the separability of these phenotypes. The cac^{H18} mutation leaves courtship song and LCRP kinetics intact. There are heteroallelic genotypes that cause aberrant courtship song and ERG transients but normal LCRP amplitude and kinetics (cac^{S}, when heterozygous with any of several *cac* lethal alleles) or aberrant kinetics but normal LCRP amplitude and normal courtship song (cac^{P73}/cac^{L6}). Similar examples exist for most of the assayed phenotypes. While the complexity of the interactions precludes a simple definition of functional classes, it is clear that the etiology of the various phenotypes must involve multiple Dmca1A functions that are at least partially separable.

Previous analyses of Dmca1A transcripts identified pairs of mutually exclusive alternative exons at two different sites and a third site that generates four transcript variants by differential inclusion of three- and six-bp exons; additional transcript complexity is thought to be generated by RNA editing at 11 identified nucleotides in the transcript (Smith *et al.* 1996, 1998; Peixoto *et al.* 1997). Functional complexity could be mediated by several mechanisms, including temporal, tissue-specific, or subcellular spatial regulation of Dmca1A expression; one imagines that at least some distinct *cac*-mediated functions might correspond directly to distinct Dmca1A isoforms. Indeed, the cac^{H18} mutation creates a stop codon within the intriguingly variant alternative exon I/IIa, indicating that Dmca1A isoforms containing this variant motif are required for normal visual function, but not for viability or normal courtship song. Additional molecular and phenogenetic analyses will continue to unravel the links between the molecular complexity and the varied and functionally separable biological functions of these Dmca1A calcium channels.

Conclusions: The *cacophony* gene of *D. melanogaster* encodes the Dmca1A calcium-channel α1 subunit protein. Phenotypic and molecular analyses of *cac* and its mutant alleles revealed that this ion-channel gene is involved in different processes important for the generation of courtship song and the regulation of normal vision. The pleiotropy associated with *cac* seems almost certainly to be explained in part by alternative splicing and the encoding of different channel isoforms within this one transcription unit. Molecular and phenogenetic analyses in the future—whereby "genetic" should include variants ranging beyond *D. melanogaster*—will further unravel the links between the gene's expression complexity and the functionally separate biological functions connected with the Dmca1A-mediated component of cellular excitability.

We thank Javier A. Arcé, Sarah Reich, and Genna Waldman for contributing to data collection; Stephen F. Goodwin and Edward Richard for discussions and critical comments on the manuscript, and Edward Doherty for assistance with photography. This work was supported by a grant from the National Institutes of Health (GM-21473). E.M.K. was supported in part by a Nathan and Bertha Richter Research Award from Brandeis University.

LITERATURE CITED

Arnon, A., B. Cook, C. Montell, Z. Selinger and B. Minke, 1997 Calmodulin regulation of calcium stores in phototransduction of *Drosophila*. Science **275:** 1119–1121.

Atkinson, N. S., G. A. Robertson and B. Ganetzky, 1991 A component of calcium-activated potassium channels encoded by the *Drosophila slo* locus. Science **253**: 551–555.

Barhanin, J., F. Lesage, E. Giullemare, M. Fink, M. Lazdunski *et al.*, 1996 K(V)LQT1 and IsK (minK) proteins associate to form the I(Ks) cardiac potassium current. Nature **384:** 78–80.

Benzer, S., 1967 Behavioral mutants of *Drosophila* isolated by countercurrent distribution. Proc. Natl. Acad. Sci. USA **58:** 1112–1119.

Bernstein, A. S., E. K. Neumann and J. C. Hall, 1992 Temporal analyses of tone pulses within the courtship songs of two sibling *Drosophila* species, their interspecific hybrid, and behavioral mutants on *D. melanogaster*. (Diptera: Drosophilidae). J. Insect Behav. **5:** 15–36.

Bülthoff, H., 1982 *Drosophila* mutants disturbed in visual orientation. Biol. Cybernet. **45:** 63–70.

Clapham, D. E., 1996 TRP is cracked but is CRAC TRP? Neuron **16:** 1069–1072.

Coombe, P. E., 1986 The large monopolar cells L1 and L2 are responsible for ERG transients in *Drosophila*. J. Comp. Physiol. A **159:** 655–665.

Coombe, P. E., and M. Heisenberg, 1986 The structural brain mutant *Vacuolar medulla* of *Drosophila melanogaster* with specific behavioral defects and cell degeneration in the adult. J. Neurogenet. **3:** 135–158.

Coyne, J. A., 1992 Genetics and speciation. Nature **355:** 511–515.

de Belle, J. S., and M. Heisenberg, 1996 Expression of *Drosophila* mushroom body mutations in alternative genetic backgrounds: a case study of the *mushroom body miniature* gene (*mbm*). Proc. Natl. Acad. Sci. USA **93:** 9875–9880.

De Waard, M., H. Liu, D. Walker, V. E. S. Scott, C. A. Gurnett *et al.*, 1997 Direct binding of G-protein βγ complex to voltage-dependent calcium channels. Nature **385:** 446–450.

Dubel, S. J., T. V. Starr, J. Hell, M. K. Ahlijanian, J. J. Enyeart, W. A. Catterall and T. P. Snutch, 1992 Molecular cloning of the α1 subunit of an omega-conotoxin-sensitive calcium channel. Proc. Natl. Acad. Sci. USA **89:** 5058–5062.

Dunlap, K., J. I. Luebke and T. J. Turner, 1995 Exocytotic Ca^{2+} channels in mammalian central neurons. Trends Neurosci. **18:** 89–98.

Dunnett, C. W., 1955 A multiple comparison procedure for comparing several treatments with a control. J. Am. Stat. Assoc. **50:** 1096–1121.

Ganetzy, B., 1996 Cysteine strings, calcium channels and synaptic transmission. BioEssays **16:** 461–463.

Gorczyca, M., and J. C. Hall, 1987 The INSECTAVOX, an integrated device for recording and amplifying courtship songs of Drosophila. Drosophila Info. Serv. **66:** 157–160.

Grabner, M., A. Bachmann, F. Rosenthal, J. Striessnig, C. Schultz *et al.*, 1994 Insect calcium channels: molecular cloning of an a1 subunit from housefly (*Musca domestica*) muscle. FEBS Lett. **339:** 189–194.

Greenspan, R. J., 1997 A kindler, gentler genetic analysis of behavior: dissection gives way to modulation. Curr. Opin. Neurobiol. **7:** 805–811.

Hall, J. C., 1994 The mating of a fly. Science **264:** 1702–1714.

Hall, J. C., L. Tompkins, C. P. Kyriacou, R. W. Siegel, F. von Schilcher *et al.*, 1980 Higher behaviors in *Drosophila* analyzed with mutations that disrupt the structure and function of the nervous system, pp. 425–455 in *Development and Neurobiology of* Drosophila, edited by O. Siddiqi, P. Babu, L. M. Hall and J. C. Hall. Plenum Press, New York.

Hall, J. C., S. J. Kulkarni, C. P. Kyriacou, Q. Yu and M. Rosbash, 1990 Genetic and molecular analysis of neural development and behavior in *Drosophila*, pp. 100–112 in *Developmental Behavioral Genetics*, edited M. E. Hahn, J. Hewitt and N. D. Henderson. Oxford University Press, New York.

Hardie, R. C., 1996 Excitation of Drosophila photoreceptors by BAPTA and ionomycin: evidence for capacitative Ca^{2+} entry. Cell Calcium **20:** 315–327.

Hardie, R. C., and B. Minke, 1993 Novel Ca2+ channels underlying transduction in *Drosophila* photoreceptors: implications for phosphoinositide-mediated Ca^{2+} mobilization. Trends Neurosci. **16:** 371–376.

Heisenberg, M., 1971 Separation of receptor and lamina potentials in the electroretinogram of normal and mutant *Drosophila*. J. Exp. Biol. **55:** 85–100.

Heisenberg, M., and K. G. Götz, 1975 The use of mutations for the partial degradation of vision in *Drosophila melanogaster*. J. Comp. Physiol. A **98:** 217–241.

Herlitze, S., D. E. Garcia, K. Mackie, B. Hille, T. Scheuer *et al.*, 1997a Modulation of Ca^{2+} channels by G-protein beta gamma subunit. Nature **380:** 258–262.

Herlitze, S., G. H. Hockerman, T. Scheuer and W. A. Catterall, 1997b Molecular determinants of inactivation and G protein modulation in the intracellular loop connecting domains I and II of the calcium channel alpha-1A subunit. Proc. Natl. Acad. Sci. USA **94:** 1512–1516.

Hille, B., 1992 *Ionic Channels of Excitable Membranes.* Sinauer, Sunderland, MA.

Hofmann, F., M. Biel and V. Flockerzi, 1994 Molecular basis for Ca^{2+} channel diversity. Annu. Rev. Neurosci. **17:** 399–418.

Homyk, T. J., and Q. Pye, 1989 Some mutations affecting neural or muscular tissues alter the physiological components of the electroretinogram in *Drosophila*. J. Neurogenet. **5:** 37–48.

Huet, F., C. Ruiz and G. Richards, 1993 Puffs and PCR: the in vivo dynamics of early gene expression during ecdysone responses in *Drosophila*. Development **118:** 613–627.

Kahn, E. S., and H. Matsumoto, 1997 Calcium/calmodulin-dependent kinase II phosphorylates *Drosophila* visual arrestin. J. Neurochem. **68:** 169–175.

Kulkarni, S. J., and J. C. Hall, 1987 Behavioral and cytogenetic analysis of the *cacophony* courtship song mutant and interacting genetic variants in *Drosophila melanogaster*. Genetics **115:** 461–475.

Lee, R. Y. N., L. Lobel, M. Hengartner, H. R. Horvitz and L. Avery, 1997 Mutations in the α1 subunit of an L-type voltage-activated Ca^{2+} channel cause myotonia in *Caenorhabditis elegans*. EMBO J. **16:** 6066–6076.

Levy, L. S., and J. E. Manning, 1981 Messenger RNA sequence complexity and homology in developmental stages of *Drosophila*. Dev. Biol. **85:** 141–149.

Lindsley, D. L., and G. G. Zimm, 1992 *The Genome of* Drosophila melanogaster. Academic Press, San Diego.

Miller, R.J., 1997 Calcium channels prove to be a real headache. Trends Neurosci. **20:** 189–192.

Minke, B., 1982 Light-induced reduction in excitation efficiency in the *trp* mutant in *Drosophila*. J. Gen. Physiol. **79:** 361–385.

Minke, B., C.-F. Wu and W. L. Pak, 1975 Induction of photoreceptor noise in the dark in a *Drosophila* mutant. Nature **258:** 84–87.

Niemeyer, B. A., E. Suzuki, K. Scott, K. Jalink and C. S. Zuker, 1996 The Drosophila light-activated conductance is composed of the two channels TRP and TRPL. Cell **85:** 651–659.

O'Connell, P. O., and M. Rosbash, 1984 Sequence, structure, and codon preference of the *Drosophila ribosomal protein 49* gene. Nucleic Acids Res. **12:** 5495–5513.

Pak, W. L., 1975 Mutations affecting the vision of *Drosophila melanogaster*, pp. 703–733 in *Handbook of Genetics, Vol. 3*, edited by R. C. King. Plenum Press, New York.

Peixoto, A. A., and J. C. Hall, 1998 Analysis of temperature-sensitive mutants reveals new genes involved in the courtship song of Drosophila. Genetics **148:** 827–838.

Peixoto, A. A., L. A. Smith and J. C. Hall, 1997 Genomic organization and evolution of alternative exons in a Drosophila calcium channel gene. Genetics **145:** 1003–1013.

Perrimon, N., L. Engstrom and A. P. Mahowald, 1984 The effects of zygotic lethal mutations on female germ-line functions in *Drosophila*. Dev. Biol. **105:** 404–414.

Perrimon, N., L. Engstrom and A. P. Mahowald, 1989 Zygotic lethals with specific maternal effect phenotypes in *Drosophila melanogaster*. I. Loci on the *X* chromosome. Genetics **121:** 333–352.

Phillips, A. M., A. Bull and L. E. Kelly, 1992 Identification of a Drosophila gene encoding a calmodulin-binding protein with homology to the *trp* phototransduction gene. Neuron **8:** 631–642.

Pragnell, M., W. M. De, Y. Mori, T. Tanabe, T. P. Snutch *et al.*, 1994 Calcium channel beta-subunit binds to a conserved motif in the I-II cytoplasmic linker of the alpha1-subunit. Nature **368:** 67–70.

Ranganathan, R., D. M. Malicki and C. S. Zuker, 1995 Signal transduction in *Drosophila* photoreceptors. Annu. Rev. Neurosci. **18:** 283–317.

Rendahl, K. G., K. R. Jones, S. J. Kulkarni, S. H. Bagully and J. C. Hall, 1992 The *dissonance* mutation at the *no-on-transient-A* locus of *D. melanogaster*: genetic control of courtship song and visual behaviors by a protein with putative RNA-binding motifs. J. Neurosci. **12:** 390–407.

Ritchie, M. G., and C. P. Kyriacou, 1994 Genetic variability of courtship song in a population of *Drosophila melanogaster*. Anim. Behav. **48:** 425–434.

Sanguinetti, M. C., M. E. Curran, A. Zou, J. Shen, P. S. Spector *et al.*, 1996 Coassembly of K(V)LQT1 and minK (Isk) proteins to form cardiac I(Ks) potassium channel. Nature **384:** 80–83.

SAS Institute, Inc., 1994. *JMP Statistics and Graphics Guide*. SAS Institute, Inc., Cary, NC.

Schafer, W. R., and C. J. Kenyon, 1995 A calcium-channel homologue required for adaptation to dopamine and serotonin in *Caenorhabditis elegans*. Nature **375:** 73–78.

Schilcher, F. V., 1976 The behavior of *cacophony*, a courtship song mutant in *Drosophila melanogaster*. Behav. Biol. **17:** 187–196.

Schilcher, F. V., 1977 A mutation which changes courtship song in *Drosophila melanogaster*. Behav. Genet. **7:** 251–259.

Simpson, L., and R. B. Emeson, 1996 RNA editing. Annu. Rev. Neurosci. **19:** 27–52.

Smith, L. A., X. Wang, A. A. Peixoto, E. K. Neumann, L. M. Hall *et al.*, 1996 A *Drosophila* calcium channel α1 subunit gene maps to a genetic locus associated with behavioral and visual defects. J. Neurosci. **16:** 7868–7879.

Smith, L. A., A. A. Peixoto and J. C. Hall, 1998 RNA editing in the *Drosophila* Dmca1A calcium-channel α1 subunit transcript. J. Neurogenet. In press.

Snutch, T. P., W. J. Tomlinson, J. P. Leonard and M. M. Gilbert, 1991 Distinct calcium channels are generated by alternative splicing and are differentially expressed in the mammalian CNS. Neuron **7:** 45–57.

Sokal, R. R., and F. J. Rohlf, 1995 *Biometry*, Ed. 2. W. H. Freeman and Co., New York.

Soong, T. W., A. Stea, C. D. Hodson, S. J. Dubel, S. R. Vincent and T. P. Snutch, 1993 Structure and functional expression of a member of the low voltage-activated calcium channel family. Science **260:** 1133–1136.

Stea, A., T. W. Soong and T. P. Snutch, 1995 Voltage-gated ion channels, pp. 114–151 in *Ligand- and Voltage-Gated Ion Channels*, edited by R. North. CRC Press, Boca Raton, FL.

Takumi, T., H. Ohkubo and S. Nakanishi, 1988 Cloning of a membrane protein that induces a slow voltage-gated potassium current. Science **242:** 1042–1045.

Tanabe, T., H. Takeshima, A. Mikami, V. Flockerzi, H. Takahashi, K. Kangawa, M. Kojima, H. Matsuo, T. Hirose and S. Numa,

1987 Primary structure of the receptor for calcium channel blockers from skeletal muscle. Nature **328:** 313–318.

Wang, K. W., K. K. Tai and S. A. Goldstein, 1996 MinK residues line a potassium channel pore. Neuron **16:** 571–577.

Wheeler, D. A., S. J. Kulkarni, D. A. Gailey and J. C. Hall, 1989 Spectral analysis of courtship songs in behavioral mutants of *Drosophila melanogaster*. Behav. Genet. **19:** 503–528.

Williams, M. E., D. H. Feldman, A. F. McCue, R. Brenner, G. Velicelebi, S. B. Ellis and M. M. Harpold, 1992 Structure and functional expression of α1, α2, and β subunits of a novel human neuronal calcium channel subtype. Neuron **8:** 71–84.

Wilson, G. G., A. Sivaprasadarao, J. B. C. Findlay and D. Wray, 1994 Changes in activation gating of IsK potassium currents brought about by mutations in the transmembrane sequence. FEBS Lett. **353:** 251–254.

Wu, C.-F., and B. Ganetzky, 1992 Neurogenetic studies of ion channels in Drosophila. pp. 261–314 in *Ion Channels, Vol. 3*, edited by T. Narahashi. Plenum Press, New York.

Zamponi, G. W., E. Bourinet, D. Nelson, J. Nargeot and T. P. Snutch, 1997 Crosstalk between G proteins and protein kinase C mediated by the calcium channel alpha1 subunit. Nature **385:** 442–446.

Zhang, J.-F., P. T. Ellinor, R. W. Aldrich and R. W. Tsien, 1996 Multiple structural elements in voltage-dependent Ca^{2+} channels support their inhibition by G proteins. Neuron **17:** 991–1003.

Zheng, W., G. Feng, D. Ren, D. F. Eberl, F. Hannan *et al.*, 1995 Cloning and characterization of a calcium channel α1 subunit from *Drosophila melanogaster* with similarity to the rat brain type D isoform. J. Neurosci. **15:** 1132–1143.

Zuker, C. S., 1996 The biology of vision in *Drosophila*. Proc. Natl. Acad. Sci. USA **93:** 571–576.

Communicating editor: C.-I Wu